Synthesis, Structures, Bonding, and Ethylene Reactivity of Group 4 Metal Alkyl Complexes Incorporating 8-Quinolinolato Ligands

Xiaohong Bei, Dale C. Swenson, and Richard F. Jordan*

Department of Chemistry, The University of Iowa, Iowa City, Iowa 52242

Received March 24, 1997[⊗]

This contribution describes the synthesis, structures, bonding, and reactivity of neutral $(Ox)_2MR_2$ and cationic $(Ox)_2MR^+$ zirconium and hafnium alkyl complexes which contain substituted 8-quinolinolato ligands (Ox^- = 2-Me-8-quinolinolato, $MeOx^-$, **2**; 2-Me-5,7-Br_2-8-quinolinolato, $MeBr_2Ox^-$, **3**). Alkane elimination and halide displacement reactions provide routes to $(MeOx)_2ZrR_2$ (**9a**, R = CH_2Ph; **9b**, R = CH_2CMe_3; **9c**, R = CH_2SiMe_3), $(MeOx)_2Hf(CH_2Ph)_2$ (**10a**), $(MeBr_2Ox)_2ZrR_2$ (**11a**, R = CH_2Ph; **11b**, R = CH_2CMe_3), $(MeBr_2Ox)_2Hf(CH_2Ph)_2$ (**14a**), $(MeOx)_2ZrCl_2$ (**15**), $(MeBr_2Ox)_2ZrCl_2$ (**16**), and $(MeBr_2Ox)_2Zr(NMe_2)_2$ (**17**). The reaction of **16**, **17**, or $(MeBr_2Ox)_4Zr$ with $AlMe_3$ yields $(MeBr_2Ox)AlMe_2$ (**18**). An X-ray crystallographic analysis shows that in the solid state **9a** adopts a distorted octahedral structure with a *trans*-O, *cis*-N, *cis*-R ligand arrangement and that one of the benzyl ligands is bonded in an η^2-fashion. Solution NMR data are consistent with this structure and establish that exchange of the distorted and normal benzyl ligands is rapid on the NMR time scale. Solution NMR data for the other $(Ox)_2MR_2$ complexes are consistent with analogous octahedral, *trans*-O, *cis*-N, *cis*-R structures for these species. Variable-temperature NMR studies establish that $(Ox)_2MR_2$ complexes undergo inversion of metal configuration (i.e., Λ/Δ isomerization, racemization) on the NMR time scale at elevated temperatures ($\Delta G^‡$ (racemization) = 15−18 kcal/mol). Thermolysis of **11a** results in migration of a benzyl ligand from Zr to C2 of a $MeBr_2Ox^-$ ligand, yielding $(MeBr_2Ox)$(2-Me-2-CH_2Ph-5,7-Br_2-Ox)$ZrCH_2Ph$ (**19**) as a single diastereomer. Reaction of **9a** or **9b** with $[HNMe_2Ph][B(C_6F_5)_4]$ yields the base-free cationic complexes $[(MeOx)_2Zr(R)][B(C_6F_5)_4]$ (**20a**, R = CH_2Ph; **20b**, R = CH_2CMe_3), while the corresponding reaction of **11a** yields the labile amine adduct $[(MeBr_2Ox)_2Zr(CH_2Ph)(NMe_2Ph)][B(C_6F_5)_4]$ (**21a**). The reaction of $[HNMePh_2][B(C_6F_5)_4]$ with the appropriate $(Ox)_2M(CH_2Ph)_2$ complex yields **20a**, $[(MeOx)_2Hf(CH_2Ph)][B(C_6F_5)_4]$ (**22a**), or $[(MeBr_2Ox)_2M(CH_2Ph)][B(C_6F_5)_4]$ (**23a**, M = Zr; **24a**, M = Hf). An X-ray crystallographic analysis establishes that the cation of **23a** adopts a square pyramidal structure with a highly distorted (η^2) benzyl ligand in the apical site and a *trans*-O, *trans*-N ligand arrangement in the basal sites, and NMR studies show that **23a** and **24a** adopt analogous structures in solution. In contrast, NMR studies establish that **20a**, **20b**, and **22a**, which contain the more strongly electron-donating $MeOx^-$ ancillary ligand, adopt distorted square pyramidal structures with an apical-O, *cis*-N ligand arrangement which allows maximum O−M π-donation. The reactions of **23a** or **24a** with PMe_3 yield the adducts $[(MeBr_2Ox)_2M(CH_2Ph)(PMe_3)][B(C_6F_5)_4]$ (**25a**, M = Zr; **26a**, M = Hf), which adopt *trans*-O, *cis*-N, *cis*-benzyl/PMe_3 structures analogous to those of the $(Ox)_2MX_2$ complexes. The $(MeBr_2Ox)_2M(\eta^2\text{-}CH_2Ph)^+$ cations **23a** and **24a** exhibit moderate ethylene polymerization activity, while the $MeOx^-$ analogues **20a** and **20b** are inactive.

Introduction

Cationic group 4 metallocene alkyl complexes Cp_2MR^+ (**1**, M = Ti, Zr, Hf; Chart 1) have been studied extensively because of their importance in olefin polymerization and other stoichiometric and catalytic processes.[1,2] These species are highly reactive because (i) the cationic, d^0, 14-electron metal center is very electrophilic and can coordinate and activate/polarize a wide variety of substrates,[3] (ii) the M−C bond is polarized and the hydrocarbyl group is very nucleophilic, and (iii) the bent-metallocene structure restricts coordination of substrates/ligands to sites which are *cis* to the M−R group. Together, these features lead to a rich insertion and σ-bond metathesis chemistry. We are interested in exploring the chemistry of new d^0 metal alkyl complexes which incorporate these properties but contain non-cyclopentadienyl ancillary ligands to determine the extent to which the reactivity patterns observed for $Cp_2M(R)^+$ species extend to other systems, probing how ligand properties and metal geometries influence reactivity, and developing new catalysts. A

(1) For olefin polymerization catalyzed by group 4 metallocene complexes, see: (a) Jordan, R. F. *Adv. Organomet. Chem.* **1991**, *32*, 325. (b) Guram, A. S.; Jordan, R. F. In *Comprehensive Organometallic Chemistry*, 2nd ed.; Lappert, M. F., Ed.; Pergamon: Oxford, 1995; Vol. 4, pp 589−625. (c) Brintzinger, H. H.; Fischer, D.; Mülhaupt, R.; Rieger, B.; Waymouth, R. M. *Angew. Chem., Int. Ed. Engl.* **1995**, *34*, 1143. (d) Bochmann, M. *J. Chem. Soc., Dalton trans.* **1996**, 255. (e) Marks, T. J. *Acc. Chem. Res.* **1992**, *25*, 57. (f) Horton, A. D. *Trends Polym. Sci.* **1994**, *2*, 158. (g) Möhring, P. C.; Coville, N. J. *J. Organomet. Chem.* **1994**, *479*, 1.

[⊗] Abstract published in *Advance ACS Abstracts,* July 1, 1997.

S0276-7333(97)00235-5 CCC: $14.00

Chart 1

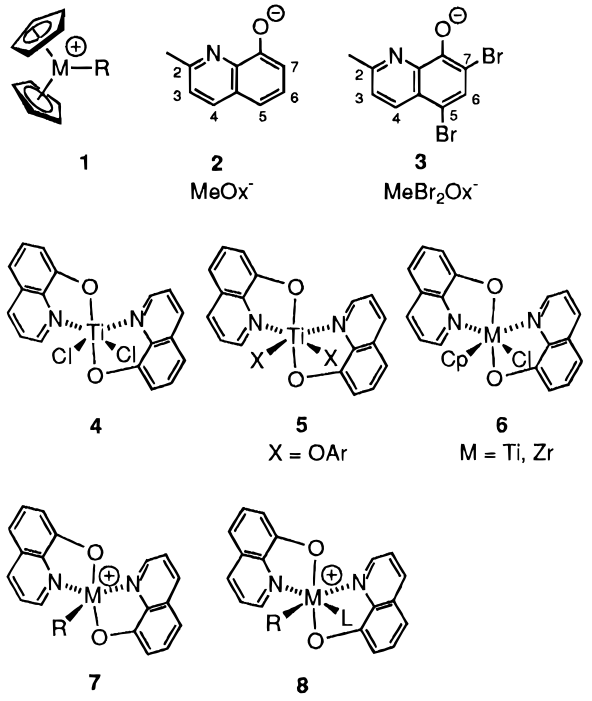

variety of non-Cp ancillary ligands have been explored in this context in recent years, including, for example, tetraazaannulenes, porphyrins, and other N_4-macrocycles,[4,5] acen, salen, and other N_2O_2 Schiff bases,[6] bidentate N,O-ligands, such as hydroxyphenyloxazolinato,[7] linked Cp−amido ligands, including $Cp(CH_2)_nNR^{2-}$ and $CpSiR_2NR^{2-}$,[8] alkoxides and chelating alkoxides,[9] $RNCRNR^-$ amidinate ligands,[10] amides and chelating bisamides,[11] boratabenzene,[12] borollides,[13] dicarbollide and related carboranyl ligands,[14] and trimethylenemethanes.[15] Here, we describe the chemistry of new group 4 metal alkyl complexes incorporating 8-quinolinolato ligands **2** and **3** (Chart 1).

Bis(8-quinolinolato) group 4 metal compounds of general type $(Ox)_2MX_2$ (**4**−**6** in Chart 1; X = Cl, OR,

(2) For other reactions involving group 4 metallocene complexes, see: (a) Rodewald, S.; Jordan, R. F. *J. Am. Chem. Soc.* **1994**, *116*, 4491. (b) Guram, A. S.; Jordan, R. F. *J. Org. Chem.* **1993**, *58*, 5595. (c) Guram, A. S.; Guo, Z.; Jordan, R. F. *J. Am. Chem. Soc.* **1993**, *115*, 4902. (d) Guram, A. S.; Jordan, R. F. *J. Org. Chem.* **1992**, *57*, 5994. (e) Guram, A. S.; Swenson, D. C.; Jordan, R. F. *J. Am. Chem. Soc.* **1992**, *114*, 8991. (f) Guram, A. S.; Jordan, R. F. *Organometallics* **1991**, *10*, 3470. (g) Guram, A. S.; Jordan, R. F.; Taylor, D. F. *J. Am. Chem. Soc.* **1991**, *113*, 1833. (h) Jordan, R. F.; Guram, A. S. *Organometallics* **1990**, *9*, 2116. (i) Jordan, R. F.; Taylor, D. F. *J. Am. Chem. Soc.* **1989**, *111*, 778. (j) Hong, Y.; Kuntz, B. A.; Collins, S. *Organometallics* **1993**, *12*, 964. (k) Hong, Y.; Norris, D.; Derek, J.; Collins, S. *J. Org. Chem.* **1993**, *58*, 3591. (l) Collins, S.; Ward, D. G. *J. Am. Chem. Soc.* **1992**, *114*, 5460. (m) Collins, S.; Koene, B. E.; Ramachandran, R.; Taylor, N. J. *Organometallics* **1991**, *10*, 2092. (n) Tjaden, E. B.; Casty, G. L.; Stryker, J. M. *J. Am. Chem. Soc.* **1993**, *115*, 9814. (o) Suzuki, K.; Maeta, H.; Matsumoto, T. *Tetrahedron Lett.* **1989**, *30*, 4853. (p) Suzuki, K.; Maeta, H.; Matsumoto, T.; Tsuchihashi, G. *Tetrahedron Lett.* **1988**, *29*, 3571. (q) Maeta, H.; Suzuki, K. *Tetrahedron Lett.* **1992**, *33*, 5969. (r) Wipf, P.; Xu, W. *J. Org. Chem.* **1993**, *58*, 825.

(3) (a) Wu, Z.; Jordan, R. F.; Petersen, J. L. *J. Am. Chem. Soc.* **1995**, *117*, 5867. (b) Guo, Z.; Swenson, D. C.; Guram, A. S.; Jordan, R. F. *Organometallics* **1994**, *13*, 766. (c) Alelyunas, Y. W.; Guo, Z.; LaPointe, R. E.; Jordan, R. F. *Organometallics* **1993**, *12*, 544. (d) Jordan, R. F.; Bradley, P. K.; Baenziger, N. C.; LaPointe, R. E. *J. Am. Chem. Soc.* **1990**, *112*, 1289

(4) (a) Black, D. G.; Swenson, D. C.; Jordan, R. F.; Rogers, R. D. *Organometallics* **1995**, *14*, 3539. (b) Uhrhammer, R.; Black, D. G.; Gardner, T. G.; Olsen, J. D.; Jordan, R. F. *J. Am. Chem. Soc.* **1993**, *115*, 8493. (c) Giannini, L.; Solari, E.; De Angelis, S.; Ward, T, R.; Floriani, C.; Chiesi-Villa, A.; Rizzoli, C. *J. Am. Chem. Soc.* **1995**, *117*, 5801 and references therein. (d) De Angelis, S.; Solari, E.; Gallo, E.; Floriani, C.; Chiesi-Villa, A.; Rizzoli, C. *Inorg. Chem.* **1992**, *31*, 2520. (e) Floriani, C.; Ciurli, S.; Chiesi-Villa, A.; Guastini, C. *Angew. Chem., Int. Ed. Engl.* **1987**, *26*, 70. (f) Cotton, F. A.; Czuchajowska, J. *Polyhedron* **1990**, *9*, 2553.

(5) (a) Brand, H.; Capriotti, J. A.; Arnold, J. *Organometallics* **1994**, *13*, 4469. (b) Brand H.; Arnold, J. *Organometallics* **1993**, *12*, 3655. (c) Brand, H.; Arnold, J. *J. Am. Chem. Soc.* **1992**, *114*, 2266. (d) Shibata, K.; Aida, T.; Inoue, S. *Chem. Lett.* **1992**, 1173. (e) Shibata, K.; Aida, T.; Inoue, S. *Tetrahedron Lett.* **1992**, *33*, 1077.

(6) (a) Tjaden, E. B.; Swenson, D. C.; Jordan, R. F. *Organometallics* **1995**, *14*, 371. (b) Solari, E.; Floriani, C.; Chiesi-Villa, A.; Rizzoli, C. *J. Chem. Soc., Dalton trans.* **1992**, 367. (c) Corazza, F.; Solari, E.; Floriani, C.; Chiesi-Villa, A.; Guastini, C. *J. Chem. Soc., Dalton trans.* **1990**, 1335. (d) Mazzanti, M.; Rosset, J. M.; Floriani, C.; Chiesi-Villa, A.; Guastini, C. *J. Chem. Soc., Dalton trans.* **1989**, 953. (e) Floriani, C. *Polyhedron* **1989**, 8, 1717.

(7) (a) Cozzi, P. G.; Gallo, E.; Floriani, C.; Chiesi-Villa, A.; Rizzoli, C. *Organometallics* **1995**, *14*, 4994. (b) Cozzi, P. G.; Floriani, C.; Chiesi-Villa, A.; Rizzoli, C. *Inorg. Chem.* **1995**, *34*, 2921. (c) Cozzi, P. G.; Floriani, C. *J. Chem. Soc., Perkin trans. 1* **1995**, 2557.

(8) (a) Hughes, A. K.; Meetsma, A.; Teuben, J. H. *Organometallics* **1993**, *12*, 1936. (b) Canich, J. M. European Patent 420436, 1991. (c) Canich, J. M.; Hlatky, G. G.; Turner, H. W. U.S. Patent 542236, 1990. (d) Stevens, J. C.; Timmers, F. J.; Wilson, D. R.; Schmidt, G. F.; Nickias, P. N.; Rosen, R. K.; Knight, G. W.; Lai, S. European Patent 416815, 1990. (e) Campbell, R. E., Jr. U.S. Patent 5066741, 1991. (f) LaPointe, R. E. European Patent 468651, 1991. (g) Devore, D. D.; Timmers, F. J.; Hasha, D. L.; Rosen, R. K.; Marks, T. J.; Deck, P. A.; Stern, C. L. *Organometallics* **1995**, *14*, 3132. (h) du Plooy, K. E.; Moll, U.; Wocadlo, S.; Massa, W.; Okuda, J. *Organometallics* **1995**, *14*, 3129. For related Sc complxes, see: (i) Shapiro, P. J.; Cotter, W. D.; Schaefer, W. P.; Labinger, J. A.; Bercaw, J. E. *J. Am. Chem. Soc.* **1994**, *116*, 4623. (j) Shapiro, P. J.; Bunnel, E.; Schaefer, W. P.; Bercaw, J. E. *Organometallics* **1990**, *9*, 867. (k) Carpenetti, D. W.; Kloppenburg, L.; Kupec, J. T.; Petersen, J. L. *Organometallics* **1996**, *15*, 1572. (l) Kloppenburg, L.; Petersen, J. L. *Organometallics* **1996**, *15*, 7.

(9) (a) van der Linden, A.; Schaverien, C. J.; Meijboom, N.; Ganter, C.; Orpen, A. G. *J. Am. Chem. Soc.* **1995**, *117*, 3008. (b) Scheverien, C. J.; Van Der Linden, A. J. *Polym. Prepr. (Am. Chem. Soc., Div. Polym. Chem.)* **1994**, *35*, 672. (c) Miyatake, T.; Mizunuma, K.; Seki, Y.; Kakugo, M. *Makromol. Chem., Rapid Commun.* **1989**, *10*, 349. (d) Kakugo, M; Miyatake, T.; Mizunuma, K.; Yagi, Y. U.S. Patent 5043,-408. (e) Miyatake, T.; Mizunuma, K.; Kakugo, M. *Makromol. Chem., Macromol Symp.* **1993**, *66*, 203. (f) Reiger, B. *J. Organomet. Chem.* **1991**, *420*, C17. (g) Fandos, R.; Meetsma, A.; Teuben, J. H. *Organometallics* **1991**, *10*, 59. (h) Fandos, R.; Teuben, J. H.; Helgesson, G.; Jagner, S. *Organometallics* **1991**, *10*, 1637.

(10) (a) Flores, J. C.; Chien, J. C. W.; Rausch, M. D. *Organometallics* **1995**, *14*, 1827. (b) Hagadorn, J. R.; Arnold, J. *Organometallics* **1994**, *13*, 4670. (c) Chernega, A. N.; Gómez, R.; Green, M. L. H. *J. Chem. Soc., Chem. Commun.* **1993,** 1415. (d) Gómez, R.; Duchateau, R.; Chernega, A. N.; Teuben, J. H.; Edelmann, F. T.; Green, M. L. H. *J. Organomet. Chem.* **1995**, *491*, 153. (e) Gómez, R.; Duchateau, R.; Chernega, A. N.; Meetsma, A.; Edelmann, F. T.; Teuben, J. H.; Green, M. L. H. *J. Chem. Soc., Dalton trans.* **1995**, 217. (f) Gómez, R.; Green, M. L. H.; Haggitt, J. L. *J. Chem. Soc., Dalton trans.* **1996**, 939. (g) Herskovics-Korine, D.; Eisen, M. S. *J. Organomet. Chem.* **1995**, *503*, 307. (h) Walther, D.; Fischer, R.; Görls, H.; Koch, J.; Schweder, B. *J. Organomet. Chem.* **1996**, *508*, 13. (i) Roesky, H. W.; Meller, B.; Noltemeyer, M.; Schmidt, H.-G.; Scholz, U.; Scheldrick, G. M. *Chem. Ber.* **1988,** *121*, 1403.

(11) Leading references, see: (a) Scollard, J. D.; McCoville, D. H.; Vittal, J. J. *Organometallics* **1995**, *14*, 5478. (b) Cloke, F. G. N.; Geldbach, T. J.; Hitchcock, P. B.; Love, J. B. *J. Organomet. Chem.* **1996**, *506*, 343. (c) Aoyagi, K.; Gantzel, P. K.; Kalai, K.; Tilley, T. D. *Organometallics* **1996**, *15*, 923. (d) Herrmann, W. A.; Denk, M.; Albach, R. W.; Behm, J.; Herdtweck, E. *Chem. Ber.* **1991**, *124*, 683. (e) Herrmann, W. A.; Denk, M.; Scherer, W.; Klingan, F. R. *J. Organomet. Chem.* **1993**, *444*, C21. (f) Warren, T. H.; Schrock, R. R.; Davis, W. M. *Organometallics* **1996**, *15*, 562. (g) Minhas, R. K.; Scoles, L.; Wong, S.; Gambarotta, S. *Organometallics* **1996**, *15*, 1113. (h) Horton, A. D.; de With, J. *J. Chem. Soc., Chem. Commun.* **1996**, 1375.

(12) Bazan, G. C.; Rodriguez, G.; Ashe, A. J., III; Al-Ahmad, S.; Müller, C. *J. Am. Chem. Soc.* **1996**, *118*, 2291.

(13) Quan, R. W.; Bazan, G. C.; Kiely, A. F.; Schaefer, W. P.; Bercaw, J. E. *J. Am. Chem. Soc.* **1994**, *116*, 4489.

(14) (a) Crowther, D. J.; Swenson, D. C.; Jordan, R. F. *J. Am. Chem. Soc.* **1995**, *117*, 10403. (b) Crowther, D. J.; Baenziger, N. C.; Jordan, R. F. *J. Am. Chem. Soc.* **1991**, *113*, 1455. (c) Crowther, D. J.; Jordan, R. F. *Makromol. Chem., Macromol. Symp.* **1993**, *66*, 121. (d) Kreuder, C.; Jordan, R. F.; Zhang, H. *Organometallics* **1995**, *14*, 2993. (e) Bowen, D. E.; Jordan, R. F.; Rogers, R. D. *Organometallics* **1995**, *14*, 3630. (f) Siriwardane, U.; Zhang, H.; Hosmane, N. S. *J. Am. Chem. Soc.* **1990**, *112*, 9637. (g) Hosmane, N. S.; Wang, Y.; Zhang, H; Maguire, J. A.; Waldhör, E.; Kaim, W.; Binder, H.; Kremer, R. K. *Organometallics* **1994**, *13*, 4156. (h) Thomas, C. J.; Jia, L.; Zhang, H.; Siriwardane, U.; Maguire, J. A.; Wang, Y.; Brooks, K. A.; Weiss, V. P.; Hosmane, N. S. *Organometallics* **1995**, *14*, 1365.

(15) Bazan, G. C.; Rodriguez, G.; Cleary, B. P. *J. Am. Chem. Soc.* **1994**, *116*, 2177.

Chart 2

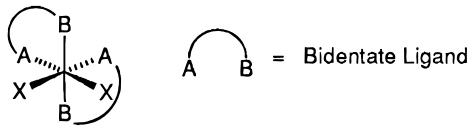

Cp; Ox^- = 8-quinolinolato) have been known for many years.[16,17] X-ray crystallographic studies established that $(Ox)_2TiCl_2$ (**4**) and $(Ox)_2Ti\{O\text{-}2,6\text{-}(^iPr)_2C_6H_3\}_2$ (**5**) adopt distorted octahedral structures with a *trans*-O, *cis*-N, *cis*-X ligand arrangement (Chart 1).[18] NMR studies of **5** showed that this C_2-symmetric structure is retained in solution, but that inversion of the metal configuration (i.e., Λ/Δ interconversion, racemization) is rapid on the NMR time scale at elevated temperatures.[19] Analogous structures have been observed for $(Ox)_2MCl(\eta^5\text{-Cp})$ (**6**; M = Ti, Zr) and high oxidation state (d^0) group 5 and group 6 complexes, such as $(Ox)_2V(=O)(O^{-i}Pr)$ and $(Ox)_2Mo(=O)_2$. However, other isomers have been observed for later transition metal (d^n, $n \neq 0$) $(Ox)_2MXX'$ complexes.[20] For example, $(MeOx)_2Ru(NO)Cl$ exists as two isomers; the $MeOx^-$ ligands adopt a *cis*-O, *trans*-N arrangement in one isomer and a *cis*-O, *cis*-N arrangement in the other.[20a–d] The $MeOx^-$ donor groups have a *cis*-O, *cis*-N arrangement in $(MeOx)_2Tc(=O)Cl$[20e] and a *cis*-O, *trans*-N arrangement in $(MeOx)_2Co(en)^+$.[20f]

These structural trends may be rationalized in terms of simple valence shell electron pair repulsion concepts as developed in detail by Kepert.[21] Analysis of donor atom−donor atom repulsions in $(bidentate)_2MX_2$ complexes (X = unidentate ligand, Chart 2) reveals that (i) the *cis*-X structures are preferred in general and (ii) donor atom−donor atom repulsions at site B are less than at site A, so that site B will be occupied by that end of an unsymmetrical bidentate ligand which forms the shortest bond to the metal. The M−O distances are significantly shorter than the M−N distances in early metal $(Ox)_2MX_2$ species, so the *trans*-O, *cis*-N, *cis*-X structure is favored. For the smaller later metals, however, the M−O and M−N distances are more similar and other isomers are observed. Additionally, electronic factors, including the *trans*-influence and π-donor properties of the ligands, are likely to influence the structures of d^0 $(Ox)_2MXX'$ complexes.

Mass spectrometric results suggest that the d^0 $(Ox)_2M$ unit is very stable. The principal fragmentation processes observed in the mass spectrum of $(Ox)_2Ti(Cl)Cp$ involve loss of Cl and/or Cp rather than disruption of the $(Ox)_2Ti$ core.[17a] In addition, Ox^- chelate ligands have been widely used as complexation agents for the quantitative analysis of transition metal ions.[22]

On the basis of these observations, we hypothesized that d^0 $(Ox)_2M(R)^+$ species of type **7** (Chart 1) should be reasonably stable and should coordinate potential substrates L *cis* to the M−R bond, yielding adducts **8**. Although it is difficult to predict whether the substrate L will be sufficiently activated to react with the M−R bond in **8**, we reasoned that the reactivity of **8** could be modified and ultimately tuned via appropriate substitution or elaboration of the Ox^- ligands. In this paper, we describe the synthesis, properties, and ethylene reactivity of zirconium and hafnium $(Ox)_2MR_2$ and $(Ox)_2M(R)^+$ complexes incorporating the 8-quinolinolato ligands $MeOx^-$ (**2**) and $MeBr_2Ox^-$ (**3**) (Chart 1).

Results and Discussion

Synthesis of $(MeOx)_2MR_2$ and $(MeBr_2Ox)_2MR_2$ Complexes (M = Zr, Hf) via Alkane Elimination. Slow addition of 2 equiv of 2-Me-8-quinolinol (MeOxH, **2**-H) to ZrR_4 (R = CH_2Ph, CH_2CMe_3, CH_2SiMe_3) in toluene or benzene results in the formation of $(MeOx)_2ZrR_2$ complexes **9a**−**c** in high yield (eq 1). Complexes

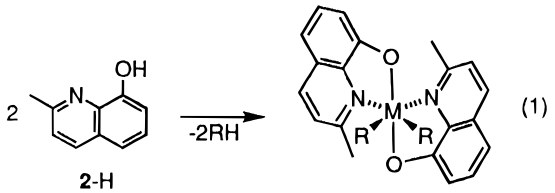

(1)

	M	R
9a	Zr	CH_2Ph
9b	Zr	CH_2CMe_3
9c	Zr	CH_2SiMe_3
10a	Hf	CH_2Ph

9a (orange) and **9b** (yellow) were obtained as pure solids by recrystallization from toluene or toluene/pentane. However, **9c** could not be recrystallized efficiently due to its high solubility in these solvents. The hafnium dibenzyl complex $(MeOx)_2Hf(CH_2Ph)_2$ (**10a**) was generated by the analogous reaction of **2**-H with $Hf(CH_2Ph)_4$.

In initial experiments, it was found that slow addition of 2 equiv of the more acidic quinolinol $MeBr_2OxH$ (**3**-H) to $Zr(CH_2Ph)_4$ in toluene results in an exothermic reaction and formation of $(MeBr_2Ox)_2Zr(CH_2Ph)_2$ (**11a**) contaminated with significant amounts of $(MeBr_2Ox)_3Zr(CH_2Ph)$ (**12**), $(MeBr_2Ox)_4Zr$ (**13**), and unreacted $Zr(CH_2$-

(16) The unsubstituted 8-quinolinolato ligand is also referred to as "oxinato" or "ox", and the methyl derivative 2-Me-8-quinolinolato (**2**) is referred to as "quinaldinate", "8-hydroxyquinaldinate", or "quin" in the literature. In this paper, "Ox" is used as a general abbreviation for substituted 8-quinolinolato ligands.

(17) (a) Charalambous, J.; Frazer, M. J.; Newton, W. E. *J. Chem. Soc. A.* **1971,** *15*, 2487. (b) Frazer, M. J.; Rimmer, B. *J. Chem. Soc. A* **1968**, 69. (c) Frazer, M. J.; Rimmer, B. *J. Chem. Soc. A.* **1968**, 2273. (d) Harrod, J. F.; Taylor, K. R. *Inorg. Chem.* **1975**, *14*, 1541.

(18) For X-ray structural studies of early transition metal d^0 $(Ox)_2MX_2$ or $(Ox)_2MXX'$ complexes, see: (a) Studd, B. F.; Swallow, A. G. *J. Chem. Soc. A.* **1968**, 1961. (b) Swallow, A. G.; Studd, B. F. *J. Chem. Soc., Chem. Commun.* **1967**, 1197. (c) Bird, P. H.; Fraser, A. R.; Lau, C. F. *Inorg. Chem.* **1973**, *12*, 1322. (d) Matthews, J. D.; Singer, N.; Swallow, A. G. *J. Chem. Soc. A.* **1970**, 2545. (e) Wang, J.; Li, J.; Gong, Y. *Chem. Res. Chin. Univ.* **1992**, *8*, 212. (f) Jeannin, Y.; Launay, J. P.; Seid Sedjadi, M. A. *J. Coord. Chem.* **1981**, *11*, 27. (g) Scheidt, W. R. *Inorg. Chem.* **1973**, *12*, 1758. (h) Atovmyan, L. O.; Sokolava, Yu. A. *J. Chem. Soc., Chem. Commun.* **1969**, 649. (i) Yamada, S.; Katayama, C.; Tanaka, J.; Tanaka, M. *Inorg. Chem.* **1984**, *23*, 253.

(19) (a) Bickley, D. G.; Serpone, N. *Inorg. Chem.* **1979**, *18*, 2200. (b) Harrod, J. F.; Taylor, K. *J. Chem. Soc., Chem. Commun.* **1971**, 696.

(20) Later transition metal (d^n, $n \neq 0$) complexes, see: (a) Kamata, Y.; Kimura, J.; Hirota, R.; Miki, E.; Mizumachi, K.; Ishimori, T. *Bull. Chem. Soc. Jpn.* **1987**, *60*, 1343. (b) Kamata, Y.; Miki, E.; Hirota, R.; Mizumachi, K.; Ishimori, T. *Bull. Chem. Soc. Jpn.* **1988**, *61*, 594. (c) Kamata, H.; Konish, Y.; Kamata, Y.; Miki, E.; Mizumachi, K.; Ishimori, T.; Nagai, T.; Tanaka, M. *Chem. Lett.* **1988**, *1*, 159. (d). Miki, E.; Masano, H.; Iwasaki, H.; Tomizawa, H.; Mizumachi, K.; Ishori, T. *Inorg. Chim. Acta* **1993**, *205*, 129. (e) Wilcox, B.; Heeg, M. J.; Deutsch, E. *Inorg. Chem.* **1984**, *23*, 2962. (f) Yamamoto, Y.; Toyota, E. *Bull. Chem. Soc. Jpn.* **1984**, *57*, 47**.**

(21) Kepert, D. L. In *Progress in Inorganic Chemistry*; Lippard, S. L., Ed.; John Wiley & Sons: New York, 1977; Vol. 23, Chapter 1.

(22) Leading references, see: (a) Phillips, J. P. *Chem. Rev.* **1956**, *56*, 271. (b) Stary, J. *The Solvent Extraction of Metal Chelates*; Pergamon: Oxford, 1964; p 80. (c) Yatirajam, V.; Arya, S. P. *Talanta* **1976**, *23*, 596. (d) Uhlemann, E.; Opitz, B.; Schilde, U. *Z. Anorg. Allg. Chem.* **1985**, *520*, 167. (e) Isshiki, K.; Tsuji, F.; Kuwamoto, T. Anal. *Chem.* **1987**, *59*, 2491.

$Ph)_4$ (eq 2).[23,24] The identities of these compounds were

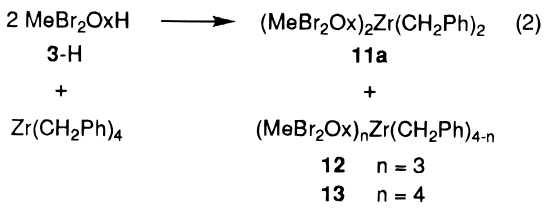

(2)

confirmed by independent synthesis from $Zr(CH_2Ph)_4$ and 3 or 4 equiv of $MeBr_2OxH$. It was subsequently determined that **11a** can be prepared free of these side products by performing the reaction at higher dilution (eq 3). The hafnium analogue **14a** was prepared in a

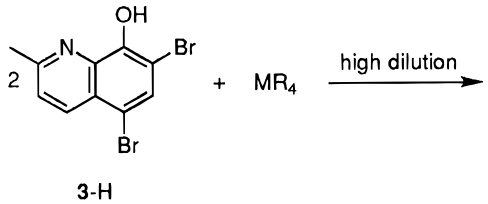

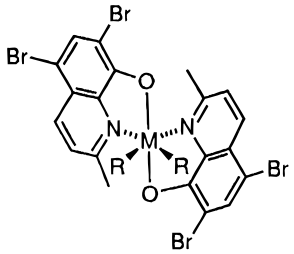
(3)

	M	R
11a	Zr	CH_2Ph
11b	Zr	CH_2CMe_3
14a	Hf	CH_2Ph

similar manner (eq 3). Complexes **11a** and **14a** were obtained as analytically pure orange solids by crystallization from toluene. Neopentyl complex **11b** was generated by the reaction of 2 equiv of $MeBr_2OxH$ (**3**-H) and $Zr(CH_2CMe_3)_4$ in hexanes.

Synthesis and Reactivity of $(MeOx)_2ZrCl_2$ and $(MeBr_2Ox)_2ZrCl_2$. The dichloride complexes $(MeOx)_2ZrCl_2$ (**15**) and $(MeBr_2Ox)_2ZrCl_2$ (**16**) are of interest as potential precursors to other $(MeOx)_2ZrR_2$ and $(MeBr_2Ox)_2ZrR_2$ species. The reaction of $ZrCl_4$ with 2 equiv of MeOxLi (**2**-Li) or $MeBr_2OxLi$ (**3**-Li) in ether generates **15** or **16** in high yield (eq 4) as yellow solids. These

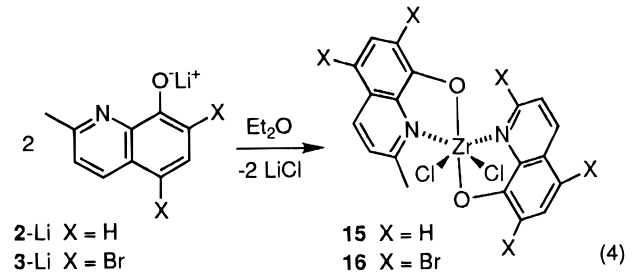

(4)

compounds are insoluble in benzene and toluene and only slightly soluble in methylene chloride and are, thus, difficult to isolate. However, **15** and **16** may be generated *in situ* and used in subsequent reactions without separation from LiCl.[25] The identities of **15** and **16** were confirmed by alternate synthesis from $[HNMe_3]Cl$ and **9a** and **11a** (eq 5).

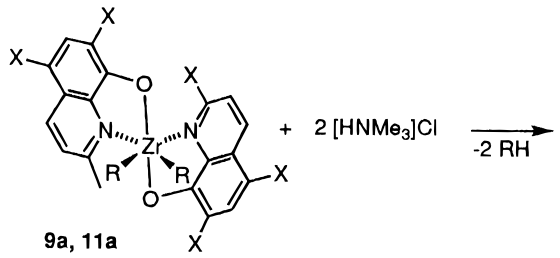

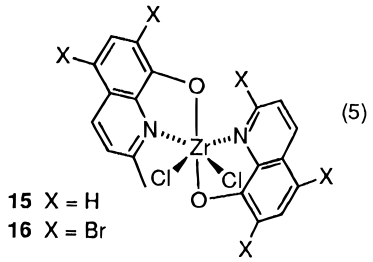
(5)

15 X = H
16 X = Br

The derivatization of **16** has been extensively investigated, as summarized in Scheme 1. The reaction of **16** and 2 equiv of $PhCH_2MgCl$ in toluene affords $(MeBr_2Ox)_2Zr(CH_2Ph)_2$ (**11a**) in good yield. Similarly, the reaction of **16** with 2 equiv of $LiNMe_2$ in Et_2O or toluene yields bis(amide) **17** cleanly.[26]

In contrast, attempts to prepare $(MeBr_2Ox)_2ZrMe_2$ by methylation of **16** were unsuccessful. The reaction of **16** and MeLi, MeMgI, or Me_2Mg gave insoluble black products, even under low-temperature conditions in toluene or toluene/ether solution (−78 to −40 °C). There is no reaction between $ZnMe_2$ and **16** in toluene at ambient temperature. The reaction of **16** and $AlMe_3$ yields the $MeBr_2Ox^-$ transfer product $(MeBr_2Ox)AlMe_2$ (**18**), which was prepared independently by the reaction of $MeBr_2OxH$ and $AlMe_3$. The parent compound $(Ox)AlMe_2$ was prepared previously and shown to be monomeric.[27] Attempts to prepare $(MeBr_2Ox)_2ZrMe_2$ from other Zr(IV) precursors were also unsuccessful. The reaction of $(MeBr_2Ox)_4Zr$ (**13**) with 2 equiv of $AlMe_3$ yields **18** and a black insoluble material, and the reaction of **17** with either 2 or 4 equiv of $AlMe_3$ yields **18** and other unidentified species.[28] These results suggest that $(MeBr_2Ox)_2ZrMe_2$ may be thermally unstable (*vide infra*).

The reactivity of **15** was only briefly investigated. Alkylation of **15** with 2 equiv of $LiCH_2CMe_3$ in C_6D_6

(23) For comparison, the pK_a of phenol and 2,4-bromophenol are 9.9 and ca. 7.7 (estimated from the values of 2,3-chlorophenol, 2,3-bromophenol, and 2,4-chlorophenol), respectively. Dean, J. A. *Handbook of Organic Chemistry*; McGraw-Hill: New York, 1987; Table 8−1.

(24) $(Ox)_4Zr$ has been characterized by X-ray diffraction. Lewis, D. F.; Fay, R. C. *J. Chem. Soc., Chem. Commun.* **1974**, 1046.

(25) The reaction of $ZrCl_4$ with **3**-Na in methylene chloride generates $(MeBr_2Ox)_4Zr$.

(26) Attempts to prepare $(MeBr_2Ox)_2Zr(NMe_2)_2$ by reaction of 2 equiv of **3**-H and $Zr(NMe_2)_4$ under a variety of conditions yielded mixtures of $(MeBr_2Ox)_nZr(NMe_2)_{4-n}$ ($n = 0 - 4$).

(27) (a) Sen, B.; White, G. L. *J. Inorg. Nucl. Chem.* **1973**, *35*, 497. (b) Sen, B.; White, G. L.; Wander, J. D. *J. Chem. Soc., Dalton trans.* **1972**, 447. (c) For related compounds, see: van Vliet, M. R. P.; van Koten, G.; de Keijser, M. S.; Vrieze, K. *Organometallics* **1987**, *6*, 1652.

(28) For the use of $AlMe_3$ as a methylation reagent for $L_nM(NMe_2)_2$ compounds, see: (a) Kim, I.; Jordan, R. F. *Macromolecules* **1996**, *29*, 489. (b) Diamond, G. D.; Jordan, R. F.; Petersen, J. L. *J. Am. Chem. Soc.* **1996**, *118*, 8024.

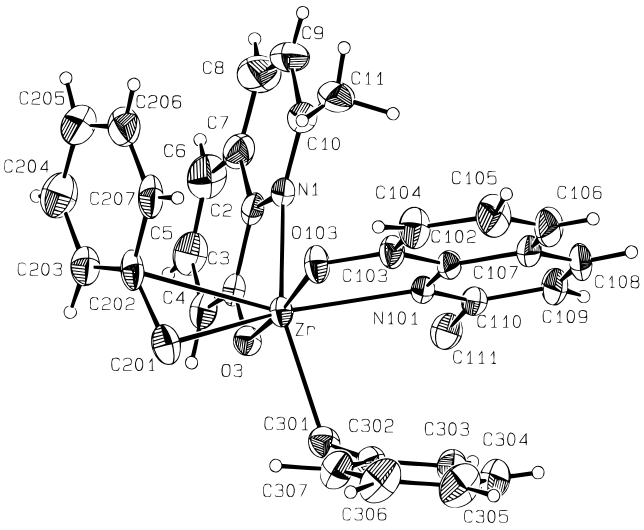

Figure 1. Molecular structure of $(MeOx)_2Zr(CH_2Ph)_2$ (**9a**).

Scheme 1

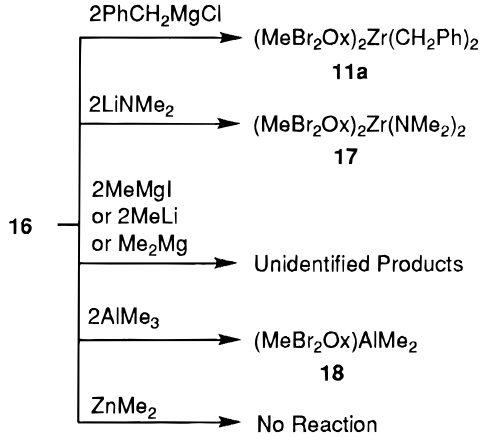

affords **9b** cleanly; however, attempted methylation of **15** with Me_2Mg yields a mixture of unidentified products (eq 6).

$$(MeOx)_2ZrCl_2 \;(\mathbf{15}) + 2\,LiCH_2CMe_3 \longrightarrow (MeOx)_2Zr(CH_2CMe_3)_2\;(\mathbf{9b}) \qquad (6)$$

X-ray Structural Analysis of $(MeOx)_2Zr(CH_2Ph)_2$ (9a). The molecular structure of $(MeOx)_2Zr(CH_2Ph)_2$ (**9a**) was determined by X-ray crystallography and is illustrated in Figure 1. Selected bond distances and angles are given in Table 1. Complex **9a** adopts a distorted octahedral structure analogous to those of **4**−**6** with a *trans*-O, *cis*-N, *cis*-benzyl ligand arrangement. The O−Zr−O bond angle (170.5(1)°) approaches the ideal O_h value. The intrachelate O−Zr−N angles are acute (O(3)−Zr−N(1), 70.70(9)°; O(103)−Zr−N(101), 70.45(9)°) due to the small $MeOx^-$ bite angle, and as a result, the remaining *trans* angles are significantly reduced from ideal O_h values (N(101)−Zr−C(201), 153.6(1)°; N(1)−Zr−C(301), 144.3(1)°). The Zr−O−C units are bent (Zr−O(3)−C(3), 125.7(2)°; Zr−O(103)−C(103), 125.9(2)°), indicating that the $MeOx^-$ oxygens are sp^2-hybridized. The Zr−O distances (Zr−O(3), 2.051(2) Å, Zr−O(103), 2.052(2)Å) are typical for Zr(IV) phenoxide compounds,[29,30] and the Zr−N bonds of **9a** (Zr−N(1), 2.450(3) Å; Zr−N(101), 2.444(3) Å) are within the range observed for other Zr(IV) pyridine complexes (2.38−2.47 Å).[29c,31] The Zr coordination geometry in **9a** is, thus, similar to that in other early metal $(Ox)_2MX_2$ complexes,[17,18] and the Zr−O and Zr−N bonding is quite normal.

Table 1. Selected Bond Distances (Å) and Bond Angles (deg) for $(MeOx)_2Zr(CH_2Ph)_2$ (9a)

Zr−C(201)	2.286(4)	Zr−N(1)	2.450(3)
Zr−C(202)	2.69	Zr−N(101)	2.444(3)
Zr−C(301)	2.293(4)	Zr−O(3)	2.051(2)
Zr−C(302)	3.20	Zr−O(103)	2.052(2)
C(201)−Zr−C(301)	91.0(2)	N(1)−Zr−N(101)	81.2(1)
C(201)−Zr−N(1)	117.7(2)	N(101)−Zr−O(3)	107.15(9)
C(201)−Zr−O(3)	96.9(1)	N(101)−Zr−O(103)	70.45(9)
C(201)−Zr−N(101)	153.6(1)	O(3)−Zr−O(103)	170.5(1)
C(301)−Zr−N(101)	80.4(1)	Zr−C(201)−C(202)	89.4(2)
C(301)−Zr−O(3)	86.0(1)	Zr−C(301)−C(302)	115.1(2)
C(301)−Zr−N(1)	144.3(1)	Zr−O(3)−C(3)	125.7(2)
N(1)−Zr−O(3)	70.70(9)	Zr−O(103)−C(103)	125.9(2)
N(1)−Zr−O(103)	99.8(1)		

While the C(301)−C(307) benzyl ligand shows normal η^1-bonding to Zr in this complex (Zr−C(301)−C(302), 115.1(2)°; Zr−C(302), 3.20Å), the C(201)−C(207) benzyl ligand is distorted such that the Zr−C(201)−C(202) angle is acute (89.4(2)°) and the Zr−C_{ipso} carbon (Zr−C(202), 2.69 Å) is short. This η^2-benzyl bonding mode results from a weak Zr···Ph π interaction and is characteristic of electron-deficient early transition metal benzyl complexes.[8a,32] Complex **9a** is formally a 16-electron species, counting the $MeOx^-$ oxygens as 4-electron (σ, π) donors and neglecting the Zr···Ph interaction. The Ph ring of the distorted benzyl ligand points toward a $MeOx^-$ pyridine ring and away from the normal benzyl ligand.

Electronic Structure of $(MeOx)_2MR_2$ Complexes. An extended Hückel molecular orbital (EHMO) analysis of the model species $(MeOx)_2ZrMe_2$ (with the same geometry as observed for **9a**) illustrates several important features of the bonding in these systems and also provides insight to the origin of the η^2-benzyl interaction.[33] As schematically illustrated in Figure 2, the two

(29) (a) Zambrano, C. H.; Profilet, R. D.; Hill, J. E.; Fanwick, P. E.; Rothwell, I. P. *Polyhedron* **1993**, *12*, 689. (b) Kresinski, R. A.; Isam, L.; Hamor, T. A.; Jones, C. J.; McCleverty, J. A. *J. Chem. Soc., Dalton trans.* **1991**, 1835. (c) Zambrano, C. H.; McMullen, A. K.; Kobriger, L. M.; Fanwick, P. E.; Rothwell, I. P. *J. Am. Chem. Soc.* **1990**, *112*, 6565. (d) Profilet, R. D.; Zambrano, C. H.; Fanwick, P. E.; Nash, J. J.; Rothwell, I. P. *Inorg. Chem.* **1990**, *29*, 4362. (e) Fanwick, P. E.; Kobriger, L. M.; McMullen, A. K.; Rothwell, I. P. *J. Am. Chem. Soc.* **1986**, *108*, 8095. (f) Chamberlain, L. R.; Durfee, L. D.; Fanwick, P. E.; Kobriger, L. M.; Latesky, S. L.; McMullen, A. K.; Steffey, B. D.; Rothwell, I. P.; Folting, K.; Huffman, J. C. *J. Am. Chem. Soc.* **1987**, *109*, 6068. (g) Latesky, S. L.; McMullen, A. K.; Niccolai, G. P.; Rothwell, I. P.; Huffman, J. C. *Organometallics* **1985**, *4*, 1896. (h) Erker, G.; Dorf, U.; Lecht, R.; Ashby, M. T.; Aulbach, M.; Schlund, R.; Kruger, C.; Mynott, R. *Organometallics* **1989**, *8*, 2037. (i) McMullen, A. K.; Rothwell, I. P.; Huffman, J. C. *J. Am. Chem. Soc.* **1985**, *107*, 1072.

(30) For discussions of M−OR bonding in early metal complexes, see: Howard, W. A.; Trnka, T. M.; Parkin, G. *Inorg. Chem.* **1995**, *34*, 5900 and references therein.

(31) (a) Howard, W. A.; Parkin, G. *J. Am. Chem. Soc.* **1994**, *116*, 606. (b) Williams, D. N.; Piarulli, U.; Floriani, C.; Chiesi-Villa, A.; Rizzoli, C. *J. Chem. Soc., Dalton trans.* **1994**, 1243. (c) Walsh, P. J.; Hollander, F. J.; Bergman, R. G. *J. Am. Chem. Soc.* **1990**, *112*, 894. (d) Walsh, P. J.; Carney, M. J.; Bergman, R. G. *J. Am. Chem. Soc.* **1991**, *113*, 6343. (e) Carney, M. J.; Walsh, P. J.; Hollander, F. J.; Bergman, R. G. *Organometallics* **1992**, *11*, 761. (f) Hoffman, D. M.; Lee, S. *Inorg. Chem.* **1992**, *31*, 2675. (g) Arnold, J.; Woo, H.-G.; Tilley, T. D. *Organometallics* **1988**, *7*, 2045. (h) Moore, E. J.; Straus, D. A.; Armantrout, J.; Santarsiero, B. D.; Grubbs, R. H.; Bercaw, J. E. *J. Am. Chem. Soc.* **1983**, *105*, 2068. (i) Peterson, E. J.; Von Dreele, R. B.; Brown, T. M. *Inorg. Chem.* **1976**, *15*, 309.

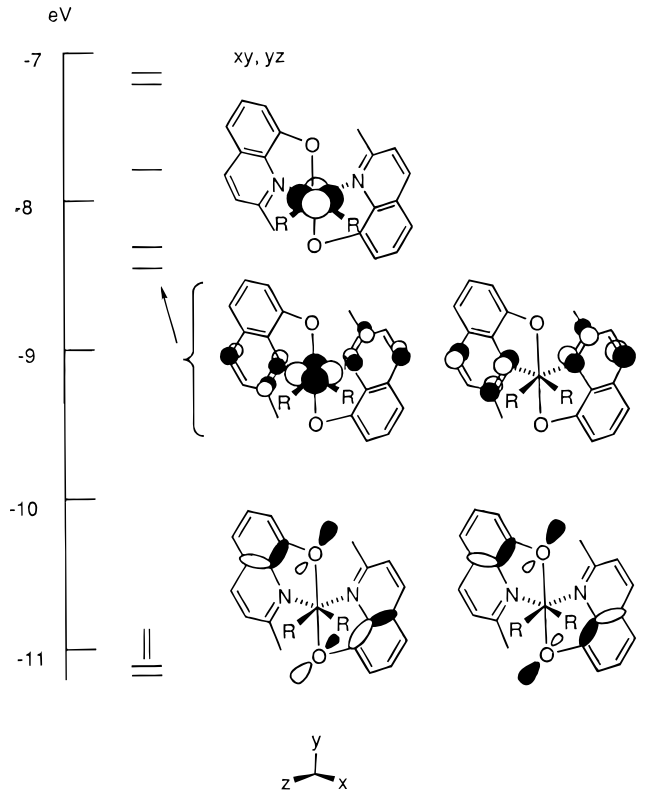

Figure 2. Schematic illustration of the frontier orbitals of the model compound $(MeOx)_2ZrMe_2$, derived from **9a** by replacement of the benzyl groups with methyl groups, as determined by an EHMO analysis.

highest occupied orbitals of $(MeOx)_2ZrMe_2$ are the $MeOx^-$ oxygen lone pair orbitals admixed with $MeOx^-$ C−C bonding orbitals. The two lowest unoccupied orbitals are $MeOx^-$-based π^* antibonding orbitals which are primarily localized on the N, C2, and C4 (see Chart 1 for numbering). These orbitals correspond to the $3b_1$ π^* orbital of pyridine[34] and also contain ca. 15% LUMO (lowest unoccupied molecular orbital) and 8% LUMO + 1 metal d character (not shown). The d_{xz} orbital lies at slightly higher energy, followed by d_{xy} and d_{yz} combinations, which are destabilized by π-donation from the $MeOx^-$ oxygens. While the precise ordering of the closely spaced unoccupied frontier orbitals is sensitive to the computational method and parameters, it is clear that these orbitals have both metal d and ligand π^* character.

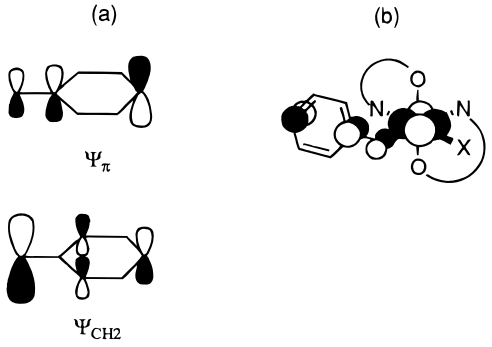

Figure 3. (a) Key frontier orbitals of the benzyl anion involved in $M-(\eta^2\text{-}CH_2Ph)$ interactions. (b) Schematic illustration of the Zr···Ph interaction in **9a**, involving overlap of the benzyl Ψ_π and Zr d_{xz} orbitals.

The key frontier orbitals of the benzyl anion which are localized on the methylene and *ipso* carbons and which interact strongly with the metal acceptor orbitals in an η^2-benzyl complex, are Ψ_{CH_2} and Ψ_π (Figure 3), which are combinations of the methylene p lone pair orbital and the phenyl HOMO (highest occupied molecular orbital).[32c,35] The $M-(\eta^2$-benzyl) bond may be considered to comprise a $M-CH_2Ph$ σ bond formed by overlap of Ψ_{CH_2} and a suitable metal σ-acceptor orbital and a Ph···M interaction resulting from overlap of Ψ_π with an empty metal d orbital. As illustrated in Figure 3b, a $(MeOx)_2Zr(\eta^2\text{-}CH_2Ph)(R)$ species (e.g., **9a**) is expected to adopt a conformation in which the η^2-benzyl phenyl group lies over a M−N bond, since this orientation maximizes overlap of the Ψ_π orbital and the metal d_{xz} acceptor orbital. This is the structure observed for **9a** in the solid state.

NMR Characterization of $(MeOx)_2MR_2$ and $(MeBr_2Ox)_2MR_2$ Complexes. The room-temperature ^1H NMR spectra of **9a**−**c**, **11a**,**b**, and **14a** each contain a single set of $MeOx^-$ or $MeBr_2Ox^-$ resonances, a single set of Ph (**9a**, **11a**, **14a**), CMe_3 (**9b**, **11b**), or $SiMe_3$ (**9c**) resonances, and an AB pattern for the MCH_2 hydrogens. These spectra are consistent with the C_2-symmetric *trans*-O, *cis*-N, *cis*-R structures shown in eqs 1−5, in which the MCH_2R hydrogens are diastereotopic due to their proximity to the chiral metal center.

The room-temperature ^1H NMR spectrum of **10a** contains a single set of $MeOx^-$ and Ph resonances and a sharp singlet rather than an AB pattern for the $HfCH_2$ hydrogens. However, as the temperature is lowered, the $HfCH_2$ singlet splits to a sharp AB pattern without intermediate broadening. The lack of broadening indicates that these line shape changes result from a change in the $\Delta\nu/J$ ratio with temperature rather than a chemical exchange process (*vide infra*), and therefore, **10a** most likely has the same solution structure as the other $(MeOx)_2MR_2$ and $(MeBr_2Ox)_2MR_2$ complexes.

The presence of one distorted and one normal benzyl ligand in the solid state structure of **9a** suggests that η^2-benzyl interactions may also be present in $(Ox)_2M(CH_2Ph)_2$ species in solution. Distorted $M-CH_2-Ph$ groups

(32) (a) Pellecchia, C.; Immirzi, A.; Pappalardo, D.; Peluso, A. *Organometallics* **1994**, *13*, 3773. (b) Bochmann, M.; Lancaster, S. J. *Organometallics* **1993**, *12*, 633. (c) Dryden, N. H.; Legzdins, P.; Trotter, J.; Yee, V. C. *Organometallics* **1991**, *10*, 2857. (d) Alelyunas, Y. W.; Jordan, R. F.; Echols, S. F.; Borkowsky, S. L.; Bradley, P. K. *Organometallics* **1991**, *10*, 1406. (e) Jordan, R. F.; LaPointe, R. E.; Baenziger, N.; Hinch, G. D. *Organometallics* **1990**, *9*, 1539. (f) Scholz, J.; Schlegel, M.; Thiele, K. H. *Chem. Ber.* **1987**, *120*, 1369. (g) Jordan, R. F.; LaPointe, R. E.; Bajgur, C. S.; Echols, S. F.; Willett, R. *J. Am. Chem. Soc.* **1987**, *109*, 4111. (h) Latesky, S. L.; McMullen, A. K.; Niccolai, G. P.; Rothwell, I. P. *Organometallics* **1985**, *4*, 902. (i) Edwards, P. G.; Andersen, R. A.; Zalkin, A. *Organometallics* **1984**, *3*, 293. (j) Girolami, G. S.; Wilkinson, G.; Thornton-Pett, M.; Hursthouse, M. B. *J. Chem. Soc., Dalton Trans.* **1984**, 2789. (k) Mintz, E. A.; Moloy, K. G.; Marks, T. J.; Day, V. W. *J. Am. Chem. Soc.* **1982**, *104*, 4692. (l) Davies, G. R.; Jarvis, J. A. J.; Kilbourn, B. T. *J. Chem. Soc., Chem. Commun.* **1971**, 1511. (m) Davies, G. R.; Jarvis, J. A. J.; Kilbourn, B. T.; Pioli, A. J. P. *J. Chem. Soc., Chem. Commun.* **1971**, 677. (n) Coles, M. P.; Dalby, C. I.; Gibson, V. C.; Clegg, W.; Elsegood, M. R. J. *J. Chem. Soc., Chem. Commun.* **1995**, 1709.

(33) The Extended Hückel calculations were performed on a CAChe system (release 3.6) using the standard parameter set provided with this system ($K = 1.75$). Very similar results were obtained using the Alverez parameters provided with this software, the principal difference being inversion of the ordering of the closely-spaced metal-based and ligand-based LUMOs.

(34) Jorgensen, W. L.; Salem, L. *The Organic Chemist's Book of Orbitals*; Academic: New York, 1973; p 263.

(35) (a) Dorigo, A. E.; Li, Y.; Houk, K. N. *J. Am. Chem. Soc.* **1989**, *111*, 6942. (b) Fleming, I. *Frontier Orbitals and Chemical Reactions*; Wiley: New York, 1976; p 55.

can be detected by ^{1}H and ^{13}C NMR spectroscopy; in particular, the reduction of the M−C−C angle and concomitant increase in H−C−H angle which results from the M···Ph interaction are manifested by reduced J_{HH} (<ca. 10 Hz) and large J_{CH} values (>ca. 125 Hz) for the MCH_2Ph group.[32,36] For example, the J_{HH} values for (EBTHI)Zr(η^1-CH_2Ph)$_2$ (EBTHI = ethylenebis(tetrahydroindenyl)) and (EBTHI)Zr(η^2-CH_2Ph)$(CH_3CN)^+$ are 11.2 and 7.1 Hz, respectively, and the J_{CH} values for $Cp_2Zr(\eta^1\text{-}CH_2Ph)_2$ and $Cp_2Zr(\eta^2\text{-}CH_2Ph)(CH_3CN)^+$ are 119 and 145 Hz, respectively.[32e,g] Zirconium benzyl complexes **9a** and **11a** exhibit $J_{CH}(CH_2)$ values (**9a**, 129 Hz; **11a**, 130 Hz) and J_{HH} values (**9a**, 8.5 Hz; **11a**, 8.8 Hz) which are intermediate between the values for the η^2-benzyl and normal benzyl ligands in the metallocene systems listed above, suggesting that the benzyl ligands in these compounds have some η^2 character in solution. The ^{1}H NMR spectra of **9a** and **11a** do not change significantly when the sample temperature is lowered to −85 °C; the *ortho*- and *meta*-Ph resonances broaden, but the $ZrCH_2$ AB pattern and the Ox^- resonances do not change. It is likely that the static structures of **9a** and **11a** contain one η^1-benzyl and one η^2-benzyl ligand, which exchange rapidly on the NMR time scale. The $HfCH_2$ J_{CH} and J_{HH} values for hafnium benzyl complexes **10a** (120, 10.2 Hz; −55 °C) and **14a** (122, 10.9 Hz) are in the range observed for normal benzyl complexes, indicating that these complexes have significantly less η^2-benzyl character than Zr analogues **9a** and **11a** and probably have η^1 structures.

The $J_{CH}(ZrCH_2)$ values for **9b** (105 Hz) and **9c** (103 Hz) are low, as typically observed in d^0 metal complexes containing CH_2CMe_3 and CH_2SiMe_3 ligands.[37] The low $J_{C_\alpha-H}$ values may result from α-agostic interactions or simply from steric interactions associated with the bulky CMe_3 or $SiMe_3$ groups, which increase the Zr−C−(C,Si) angle, leading to a small H−C−H angle and concomitantly small J_{CH} values.

Dynamic NMR Behavior of $(Ox)_2MR_2$ Complexes. It is well-documented that six-coordinate, bis(chelate) $(AA)_2MXX'$ and $(AB)_2MXX'$ complexes can undergo inversion of configuration at the metal (i.e., interconversion of Δ and Λ stereoisomers) by twist or bond-rupture mechanisms.[19,38] Serpone determined the racemization barriers for $(Ox)_2Ti\{O\text{-}2,6\text{-}(^iPr)_2C_6H_3\}_2$ ($\Delta G^‡$ (racemization) = 20.0(3) kcal/mol) and $(MeOx)_2Ti\{O\text{-}2,6\text{-}(^iPr)_2C_6H_3\}_2$ ($\Delta G^‡$ (racemization) = 17.0(3) kcal/mol) and proposed that racemization proceeds via Ti−N bond cleavage and formation of a configurationally labile five-coordinate intermediate.[19] Ti−N bond dissociation is promoted by the *ortho*-methyl substituent in $(MeOx)_2Ti\{O\text{-}2,6\text{-}(^iPr)_2C_6H_3\}_2$, resulting in the lower barrier observed in this case. Similar processes are possible for $(Ox)_2ZrR_2$ and $(Ox)_2HfR_2$ complexes. As noted above, the ^{1}H NMR spectra of **9a**−**c**, **11a**, and **14a** all exhibit AB patterns for the MCH_2 hydrogens at room temperature, which implies that racemization is slow on the NMR time scale under these conditions. To probe this issue, high-temperature spectra of **9b**, **11b**, and **14a** were investigated. In all three cases, the MCH_2 AB patterns broaden and coalesce to singlets as the temperature is raised, indicating that racemization is rapid on the NMR time scale at higher temperatures. Racemization barriers determined from these line shape changes are as follows: $\Delta G^‡$ (racemization) **9b**, 15.1(1) kcal/mol; **11b**, 15.7(1) kcal/mol; **14a**, 17.5(1) kcal/mol.[39,40] Thus, the racemization barriers are insensitive to the presence of the electron-withdrawing Br substituents on the Ox^- ligands (**9b** vs **11b**). This racemization process probably proceeds by a dissociation mechanism (eq 7).

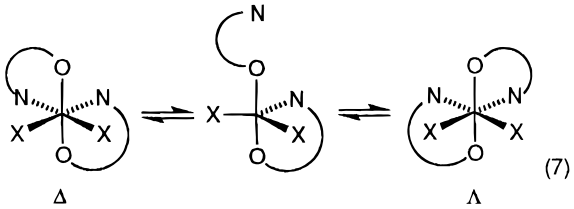

(7)

Thermal Rearrangement of $(MeOx)_2Zr(CH_2Ph)_2$. Thermolysis of **11a** results in migration of a benzyl group from Zr to C2′ of one of the $MeBr_2Ox^-$ ligands, yielding rearrangement product **19** as a single diastereomer (eq 8). This reaction is 75% complete after 1.5 h at 70 °C (toluene-d_8); however, **19** is further converted to unidentified products after more prolonged thermolysis or at higher temperatures. Complex **19** was isolated as a yellow solid.

The ^{1}H NMR spectrum of **19** was completely assigned using COSY and NOESY data and general chemical shift trends and shows that this compound has C_1 symmetry. The H3 (δ 7.15), H4 (δ 8.37), and Me (δ 2.07) resonances for one chelate ligand (the unprimed $MeBr_2O$ in eq 8) appear in the normal ranges for $(MeBr_2Ox)_2Zr$ complexes (e.g., **11a**). However, the resonances for the other N,O-ligand (the primed $MeBr_2O$ in eq 8) are unusual. The H3′ (δ 4.99) and H4′ (δ 6.74) resonances are shifted upfield into the aromatic olefin region (cf. styrene H1 δ 7.0; H2 δ 5.05, 5.35), and the $J_{H3'-H4'}$ value (9.5 Hz) is larger than the normal J_{H3-H4} values observed for $(MeBr_2Ox)_2Zr$ complexes (ca. 8.6 Hz). The

(36) Additionally, for many η^2−benzyl complexes, the *o*-Ph ^{1}H NMR resonances and the CH_2 and C_{ipso} ^{13}C NMR resonances appear at high field. However, for $(Ox)_2MR_2$ complexes, the ^{1}H NMR shifts of the *o*-Ph hydrogens may also be influenced by the ring currents of the Ox^- ligands and it is difficult to distinguish the benzyl C_{ipso} resonance from the other C_{ipso} resonances in the ^{13}C NMR spectrum. Therefore, these criteria are less useful probes of the benzyl bonding mode in $(Ox)_2M(CH_2Ph)X$ species.

(37) See discussions in the following: (a) Guo, Z.; Swenson, D. C.; Jordan, R. F. *Organometallics* **1994**, *13*, 1424. (b) Poole, A. D.; Williams, D. N.; Kenwright, A. M.; Gibson, V. C.; Clegg, W.; Hockless, D. C. R.; O'Neil, P. A. *Organometallics* **1993**, *12*, 2549. (c) Bruno, J. W.; Smith, G. M.; Marks, T. J.; Fair, C. K.; Schultz, A. J.; Williams, J. M. *J. Am. Chem. Soc.* **1986**, *108*, 40. (d) Amorose, D. M.; Lee, R. A.; Petersen, J. L. *Organometallics* **1991**, *10*, 2191.

(38) (a) Denekamp, C. I. F.; Evans, D. F.; Slawin, A. M. Z.; Williams, D. J.; Wong, C. Y.; Woollins, J. D. *J. Chem. Soc., Dalton. trans.* **1992**, 2375. (b) Gau, H.; Fay, R. C. *Inorg. Chem.* **1990**, *29*, 4974. (c) Nieto, J. L.; Galindo, F.; Gutiérrez, A. M. *Polyhedron* **1985**, *4*, 1611. (d) Willem, R.; Gielen, M.; Pepermans, H.; Brocas, J.; Fastenakel, D.; Finocchiaro, P. *J. Am. Chem. Soc.* **1985**, *107*, 1146. (e) Willem, R.; Gielen, M.; Pepermans, H.; Hallenga, K.; Recca, A.; Finocchiaro, P. *J. Am. Chem. Soc.* **1985**, *107*, 1153. (f) Holm, R. H. In *Dynamic Nuclear Magnetic Resonance Spectroscopy*; Jackman, L. M., Cotton, F. A., Eds.; Academic Press: New York, 1975; Chapter 9.

(39) (a) Racemization barriers $\Delta G^‡$ (racemization) were determined from the coalescence of the MCH_2 AB patterns using the following equations: $\Delta G^‡$ (racemization) = $4.576T_c[10.319 + \log(T_c/k_c)]$, where T_c is the coalescence temperature and k_c is the exchange rate constant at coalescence, which is given by $k_c = \pi[(\Delta\nu AB^2+6J_{AB}^2]^{1/2}/2^{1/2}$. For **9b**: $\Delta\nu_{AB}$ = 142.7 Hz, J_{AB} = 13.0 Hz, T_c = 320 K. For **11b**, $\Delta\nu_{AB}$ = 159.1 Hz, J_{AB} = 13.5 Hz, T_c = 334 K. For **14a**, $\Delta\nu_{AB}$ = 31.1 Hz, J_{AB} = 10.7 Hz, T_c = 350 K. See: (b) Alexander, S. *J. Chem. Phys.* **1962**, *37*, 971. (c) Kurland, R. J.; Rubin, M. B.; Wise, W. B. *J. Chem. Phys.* **1964**, *40*, 2426. (d) Kost, D.; Zeichner, A. *Tetrahedron. Lett.* **1974**, 4533.

(40) It was not possible to determine racemization barriers for **10a** or **11a** due to temperature-dependent $\Delta\nu/J$ ratios.

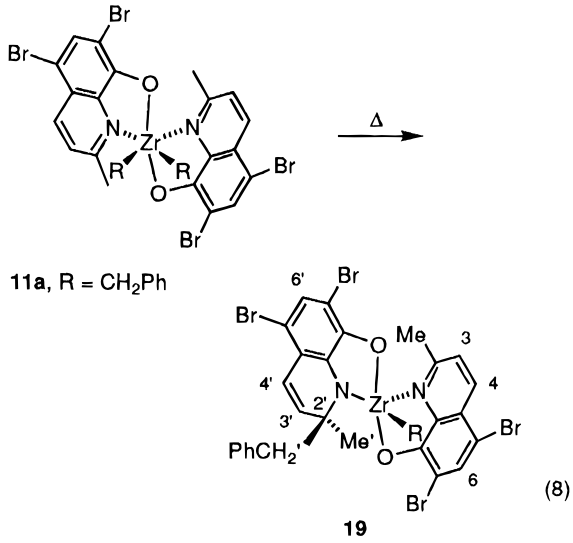

(8)

Me′ resonance is shifted upfield into the aliphatic region (δ 0.62) and is slightly broadened, suggesting the existence of long range coupling. Two AB patterns are observed for the $-CH_2$Ph groups of **19**. One set (δ 2.86, 2.84, $J_{HH} = 11.8$) is assigned to the $ZrCH_2Ph$ group. The other set consists of two more widely separated doublets (δ 3.31, 2.32, $J_{HH} = 12.5$), which are slightly broadened. Significantly, the downfield doublet of this set exhibits a COSY correlation with the Me′ group. These data are consistent with the structure proposed for **19** in eq 8, in which one benzyl group has migrated to C2′, such that CH_2Ph′/Me′ H−H coupling is possible. The ^{13}C NMR spectrum of **19** confirms this proposed structure. Two methylene ^{13}C NMR resonances are observed: one is assigned to the $ZrCH_2$Ph group on the basis of the δ(C) (73.6) and J_{CH} (116 Hz) values, which are characteristic of a normal $ZrCH_2Ph$ group. The methylene chemical shift (δ 48.3) and J_{CH} (126 Hz) values for the other benzyl group are characteristic of an organic benzyl group and consistent with the values expected for the migrated benzyl group in **19**. Additionally, a quaternary carbon resonance is observed at δ 61.5 which is assigned to C2′. The chemical shifts for the migrated CH_2Ph′ methylene carbon and C2′ agree well with the values predicted using standard ^{13}C NMR chemical shift additivity rules.[41]

The data for **19** do not allow assignment of the coordination geometry. However, the distorted trigonal bipyramidal structure shown in eq 8 is reasonable, requires minimal structural rearrangement from **11a**, and allows for effective π-donation from the amide function to the Zr $eq_\perp$ acceptor orbital.[42]

The facile migration of a benzyl group from Zr to C2′ in eq 8 reflects the nucleophilic character of the Zr−CH_2Ph group and the electrophilic character of the C2 carbons of the $MeBr_2Ox^-$ ligands. As noted above, EHMO calculations reveal that the frontier orbitals of $(MeOx)_2ZrR_2$ species include low-lying empty orbitals with significant orbital density at these carbons. This rearrangement probably involves a simple intramolecular 1,3-suprafacial migration of the benzyl group, resulting in a single diastereomer of the product. The apparent instability of $(MeOx)_2ZrMe_2$ and $(MeBr_2Ox)_2ZrMe_2$ noted above may be due to a similar but more rapid rearrangement. The rate of alkyl migration should be determined primarily by electronic factors in these sterically open systems and is, therefore, expected to vary in the order R = H > alkyl > benzyl.[4e,32d,43]

Similar rearrangements have been observed in related Zr(IV) systems. For example, Rothwell has reported that the dibenzyl complex $\{2,6\text{-}(^tBu)_2\text{-}C_6H_3O\}_2Zr(CH_2Ph)_2$(bipy) rearranges at room temperature by benzyl migration to a bipy α-carbon.[44] Interestingly the corresponding dimethyl complex does not rearrange under these conditions, which suggests that relief of steric crowding is an important driving force for this process in these sterically congested species. Tetraaza macrocycle complexes, such as $(Me_4taa)ZrMe_2$ and $(Me_4taen)ZrR_2$, rearrange by alkyl migration from Zr to a macrocycle imine carbon.[4]

Synthesis of $(Ox)_2M(R)^+$ Complexes. In initial efforts to generate $(MeOx)_2Zr(R)^+$ cations, the reactions of **9a** and **9b** with $[HNMe_2Ph][B(C_6F_5)_4]$ were investigated by ^{1}H NMR spectroscopy (eq 9).[6a,45] These reac-

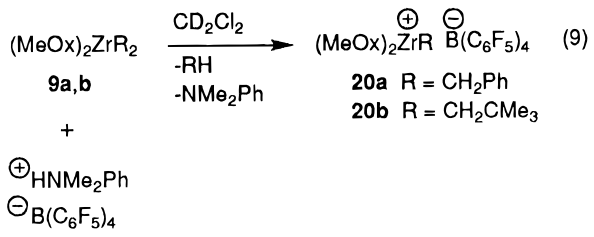

(9)

tions proceed rapidly (<10 min) and quantitatively in methylene chloride at 23 °C, yielding the base-free cations $(MeOx)_2Zr(CH_2Ph)^+$ (**20a**) and $(MeOx)_2Zr(CH_2CMe_3)^+$ (**20b**), which are described in detail below, as

(41) Chemical shifts calculated for the model compound **I** are, as follows: C2, δ 66.4; CH_2Ph, δ 44.2. These values agree well with those observed for the analogous carbons of rearrangement product **19**. Comparison of ^{13}C NMR chemical shift values for methyl groups in simple methylamines and $ZrNMe_2$ compounds shows that replacement of the N*Me* group by Zr will change δ C2 by <5 ppm. Chemical shifts were calculated using the method and parameters given in the following: Atta-Ur-Rahman, *Nuclear Magnetic Resonance*; Springer-Verlag: New York, 1986; pp 149−152.

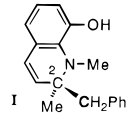

I

(42) Albright, T. A.; Burdett, J. K.; Whangbo, M. *Orbital Interactions in Chemistry*; John Wiley & Son: New York, 1985; p 320.

(43) Alelyunas, Y. W.; Guo, Z.; LaPointe, R. E.; Jordan, R. F. *Organometallics* **1993**, *12*, 544.

(44) Kobriger, L. M.; McMullen, A. K.; Fanwick, P. E.; Rothwell, I. P. *Polyhedron* **1989**, *8*, 77.

(45) For the use of HNR_3^+ reagents and the $B(C_6F_5)_4^-$ counterion in the generation of $L_nM(R)^+$ reagents, see refs 1−11 and (a) Bochmann, M.; Wilson, L. M. *J. Chem. Soc., Chem. Commun.* **1986**, 1610. (b) Lin, Z.; Le Marechal, J.; Sabat, M.; Marks, T. J. *J. Am. Chem. Soc.* **1987**, *109*, 4127. (c) Turner, H. W.; Hlatky, G. G. Eur. Pat. Appl. 0 277 003, 1988. (d) Hlatky, G. G.; Turner, H. W.; Eckman, R. R. *J. Am. Chem. Soc.* **1989**, *111*, 2728. (e) Turner, H. W. Eur. Pat. Appl. 0 277 004, 1988. (f) Hlatky, G. G.; Eckman, R. R.; Turner, H. W. *Organometallics* **1992**, *11*, 1413. (g) Eshuis, J. J. W.; Tan, Y. Y.; Meetsma, A.; Teuben, J. H.; Renkema, J.; Evens, G. G. *Organometallics* **1992**, *11*, 362. (h) Eshuis, J. J. W.; Tan, Y. Y.; Renkema, J.; Teuben, J. H. *J. Mol. Catal.* **1990**, *62*, 277. (i) Amorose, D. M.; Lee, R. A.; Petersen, J. L. *Organometallics* **1991**, *10*, 2191. (j) Horton, A. D.; Orpen, A. G. *Organometallics* **1991**, *10*, 3910. (k) Bochmann, M.; Jaggar, A. J.; Nicholls, J. C. *Angew. Chem., Int. Ed. Engl.* **1990**, *29*, 780. (l) Horton, A. D.; Frijins, J. H. G. *Angew. Chem., Int. Ed. Engl.* **1991**, *30*, 1152. (m) Grossman, R. B.; Doyle, R. A.; Buchwald, S. L. *Organometallics* **1991**, *10*, 1501. (n) Bochmann, M.; Lancaster, S. J. *J. Organomet. Chem.* **1992**, *434*, C1. (o) Ewen, J. A.; Elder, M. J.; Jones, R. L.; Haspeslagh, L.; Atwood, J. L.; Bott, S. G.; Robinson, K. *Makromol. Chem., Macromol. Symp.* **1991**, *48/49*, 253.

the $B(C_6F_5)_4^-$ salts. The amine coproduct NMe_2Ph does not coordinate to these cations at room temperature.

In contrast, the reaction of **11a** and $[HNMe_2Ph][B(C_6F_5)_4]$ yields the amine adduct $(MeBr_2Ox)_2Zr(CH_2Ph)(NMe_2Ph)^+$ (**21a**, eq 10). Below −40 °C, the ^1H NMR

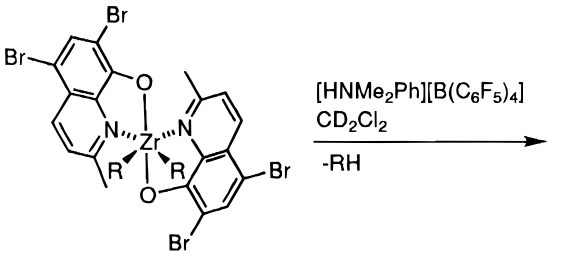

11a R = CH_2Ph

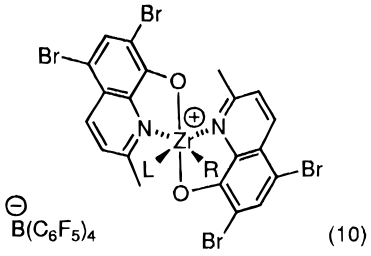

21a, L = NMe_2Ph (10)

spectra of **21a** contain two sets of $MeBr_2Ox^-$ resonances, an AB pattern for the $ZrCH_2$ unit, and two NMe_2Ph methyl resonances (1/1 intensity ratio), indicating that the coordinated NMe_2Ph does not exchange on the NMR time scale in this temperature range. However, at room temperature, broad singlets are observed for the $MeBr_2Ox^-$ and NMe_2Ph groups, indicating that amine exchange is rapid on the NMR time scale. The formation of NMe_2Ph adduct **21a** indicates that $(MeBr_2Ox)_2Zr(CH_2Ph)^+$ is a stronger Lewis acid than nonbrominated analogue **20a**, as expected due to the electron-withdrawing effect of the Br substituents. Complex **21a** decomposes at room temperature in CD_2Cl_2 and was not isolated.[46] Similarly, the reaction of **14a** with $[HNMe_2Ph][B(C_6F_5)_4]$ yields the labile amine adduct $[(MeBr_2Ox)_2Hf(CH_2Ph)(NMe_2Ph)][B(C_6F_5)_4]$.

To simplify the isolation of base-free $(Ox)_2M(R)^+$ species and to avoid the formation of amine coordination, we investigated the reactions of $(Ox)_2MR_2$ complexes with the bulkier, more acidic ammonium salt $[HNMePh_2][B(C_6F_5)_4]$ (eq 11).[6a] In benzene or toluene,

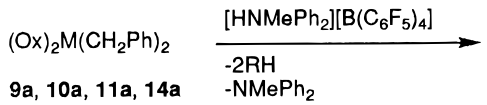

9a, **10a**, **11a**, **14a**

$(Ox)_2M(CH_2Ph)^+$ $B(C_6F_5)_4^-$

	M	Ox
20a	Zr	MeOx
22a	Hf	MeOx
23a	Zr	$MeBr_2Ox$
24a	Hf	$MeBr_2Ox$

(11)

these reactions yield $[(Ox)_2M(R)][B(C_6F_5)_4]$ salts **20a**, **20b**, **22a**, **23a**, and **24a**, which separate from the reaction mixtures as oils and can be isolated as yellow solids by separation from the supernatants, trituration with benzene, and drying under vacuum. These salts are stable in CH_2Cl_2 and were characterized by NMR spectroscopy; additionally, satisfactory elemental analyses were obtained for **22a**, **23a**, and **24a**. Recrystallization of these $[(Ox)_2MR][B(C_6F_5)_4]$ compounds is difficult due to their high solubility in chlorinated solvents and tendency to "oil out" of hydrocarbon solvents or mixtures of chlorinated and hydrocarbon solvents. However, $[(MeBr_2Ox)_2Zr(\eta^2\text{-}CH_2Ph)][B(C_6F_5)_4]$ (**23a**) was successfully recrystallized from CH_2Cl_2 and characterized by X-ray diffraction.

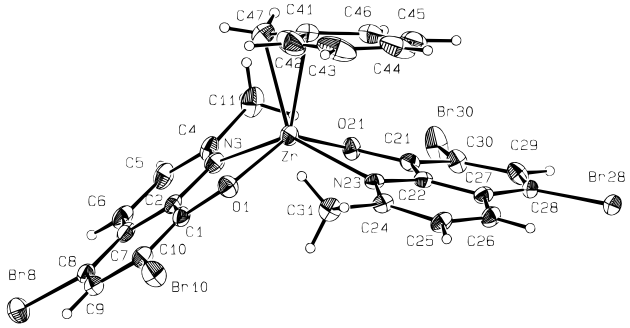

Figure 4. Molecular structure of the $(MeBr_2Ox)_2Zr(\eta^2\text{-}CH_2Ph)^+$ cation of **23a**.

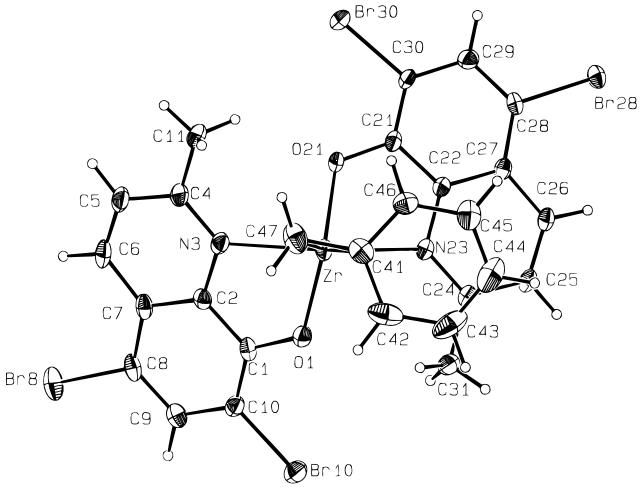

Figure 5. Alternate view of the structure of the $(MeBr_2Ox)_2Zr(\eta^2\text{-}CH_2Ph)^+$ cation of **23a**.

X-ray Structure of $[(MeBr_2Ox)_2Zr(\eta^2\text{-}CH_2Ph)][B(C_6F_5)_4]$ (23a). Complex **23a** crystallizes as discrete ions. The anion structure is normal. The molecular structure of the $(MeBr_2Ox)_2Zr(\eta^2\text{-}CH_2Ph)^+$ cation is illustrated in Figures 4 and 5, and important bond distances and angles are listed in Table 2. The $(MeBr_2Ox)_2Zr(\eta^2\text{-}CH_2Ph)^+$ cation adopts a distorted square pyramidal structure in which the η^2-benzyl ligand occupies the apical site and the $MeBr_2Ox^-$ ligands occupy the basal sites in a *trans*-O, *trans*-N arrangement. The apical−Zr−basal angles between the centroid of the C(47)−C(41) bond and the basal O and N donor atoms are all 111 ± 4°, and the *trans* O−Zr−O and N−Zr−N angles are 137.0(1)° and 138.1(1)°, respectively. The Zr−ligand distances in **23a** are 0.05−0.1 Å shorter than the corresponding distances in neutral dibenzyl complex **9a**. The η^2-benzyl ligand is

(46) The decomposition of **21a** in CD_2Cl_2 probably proceeds by the same type of mechanism as proposed for $(acen)Zr(R)(NR'_3)^+$ species. See ref 6a for details.

Table 2. Selected Bond Distances (Å) and Bond Angles (deg) for [(MeBr$_2$Ox)$_2$Zr(η^2-CH$_2$Ph)][B(C$_6$F$_5$)$_4$] (23a)

Zr−O(1)	1.992(3)	Zr−N(23)	2.353(4)
Zr−O(21)	2.006(3)	Zr−C(41)	2.448(5)
Zr−N(3)	2.340(4)	Zr−C(47)	2.245(6)
O(1)−Zr−O(21)	137.0(1)	N(3)−Zr−N(23)	138.1(1)
O(1)−Zr−N(3)	73.7(1)	N(3)−Zr−C(41)	127.6(2)
O(1)−Zr−N(23)	94.4(1)	N(3)−Zr−C(47)	92.4(2)
O(1)−Zr−C(41)	114.3(2)	N(23)−Zr−C(41)	94.1(2)
O(1)−Zr−C(47)	112.5(2)	N(23)−Zr−C(47)	128.6(2)
O(21)−Zr−N(23)	74.4(1)	Zr−C(47)−C(41)	80.0(3)
O(21)−Zr−N(3)	87.3(1)	Zr−O(1)−C(1)	123.4(3)
O(21)−Zr−C(41)	107.9(2)	Zr−O(21)−C(21)	121.0(3)
O(21)−Zr−C(47)	106.3(2)		

oriented such that the Ph ring lies over the Zr−N(23) bond (see Figure 5).

The benzyl ligand in **23a** is highly distorted, as is evident from the very acute Zr−C(47)−C(41) bond angle (80.0(3)°) and short Zr−C(41) contact (2.448(5) Å). The extent of distortion, i.e., the strength of the Zr···Ph interaction, in **23a** is clearly much greater than that in **9a**, as expected from the increased metal charge. The benzyl ligand in **23a** is significantly more distorted than those in the metallocene complexes Cp$_2$Zr(η^2-CH$_2$Ph)(CH$_3$CN)$^+$ (Zr−C−C 84.9(4)°; Zr−C$_{ipso}$, 2.648(6) Å) and *rac*-(EBTHI)Zr(η^2-CH$_2$Ph)(CH$_3$CN)$^+$ (Zr−C−C, 84.4(5)°; Zr−C$_{ipso}$, 2.627(9) Å).[32e,g] The Zr−CH$_2$ bond in **23a** (2.245(6) Å) is significantly shorter than those in Cp$_2$Zr(η^2-CH$_2$Ph)(CH$_3$CN)$^+$ (2.344(8) Å) and *rac*-(EBTHI)Zr(η^2-CH$_2$Ph)(CH$_3$CN)$^+$ (2.321(9) Å).

The structures of cation **23a** and its neutral precursor **11a** are formally related as shown in eq 12. Loss of one

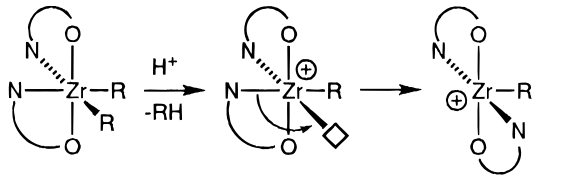

(12)

benzyl ligand generates a square pyramidal species with a MeBr$_2$Ox$^-$ nitrogen in the apical site. A simple shift of the other MeBr$_2$Ox$^-$ nitrogen by ca. 90° generates the observed structure of **23a**.

Electronic Structure of 23a. To probe the origin of the η^2-bonding mode and the orientational preference of the benzyl ligand in **23a**, the frontier orbitals of the model species (MeBr$_2$Ox)$_2$Zr(Me)$^+$ (given the same geometry as **23a**) were investigated by an EHMO analysis (Figure 6).[47] The two lowest unoccupied orbitals are MeBr$_2$Ox$^-$-based π* antibonding orbitals which are primarily localized on N, C2, and C4 (see Chart 1 for numbering) and are similar to the LUMOs of (MeOx)$_2$ZrMe$_2$ (Figure 2). Slightly above these orbitals lie the empty d$_{xy}$, d$_{xz}$, and d$_{yz}$ orbitals, the latter of which is raised in energy due to π-donation from the MeBr$_2$Ox$^-$ oxygens. Of these three acceptor orbitals, d$_{xz}$ is geometrically and energetically best suited for overlap with the benzyl Ψ_π donor orbital in the corresponding η^2-benzyl complex **23a**. The Ψ_π/d$_{xz}$ interaction is maximized when the benzyl is oriented such that the phenyl ring lies flat over a Zr−N bond. Note that that, as for (MeBr$_2$Ox)$_2$ZrMe$_2$, the precise ordering of the LUMOs is sensitive to the computational method and the parameters used.

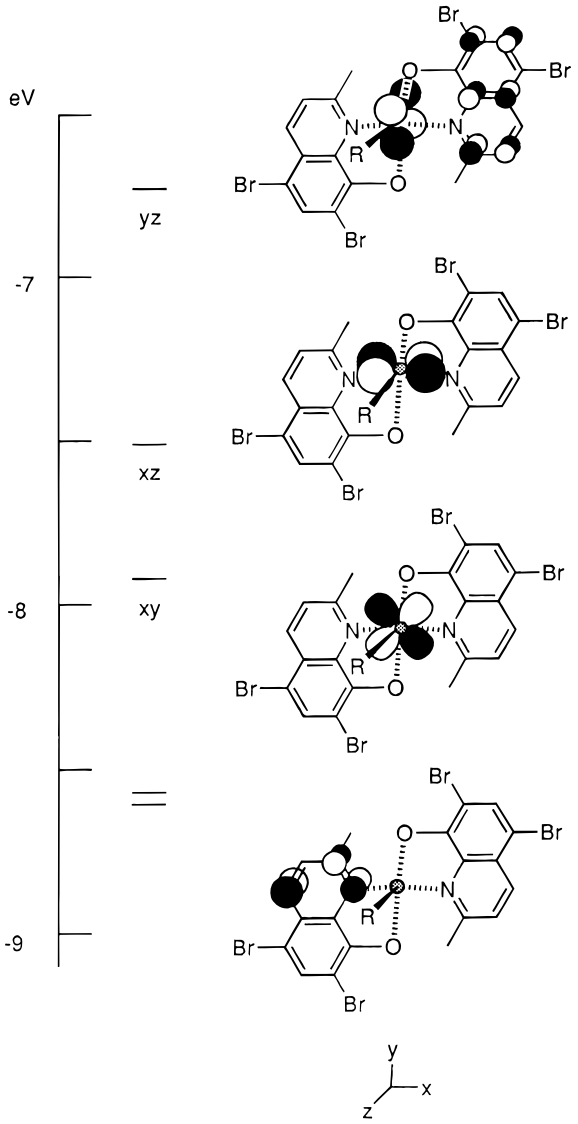

Figure 6. Schematic illustration of the frontier orbitals of the model compound (MeBr$_2$Ox)$_2$ZrMe$^+$, derived from **23a** by replacement of the benzyl phenyl ring with a hydrogen, as determined by an EHMO analysis.

Solution Structure and Dynamic Behavior of (MeBr$_2$Ox)$_2$M(CH$_2$Ph)$^+$ (M = Zr, Hf). The solution structures and dynamic behavior of (MeBr$_2$Ox)$_2$M(η^2-CH$_2$Ph)$^+$ complexes **23a** and **24a** have been probed by NMR spectroscopy. The ZrCH$_2$ J_{HH} (8.6 Hz) and J_{CH} (145 Hz) values for **23a** establish that the η^2-benzyl interaction observed in the solid state is maintained in solution. The −85 °C ^{1}H NMR spectrum of **23a** (Figures 7 and 8) contains two sets of MeBr$_2$Ox$^-$ resonances, two sets of *o*-Ph and *m*-Ph resonances, a single *p*-Ph resonance, and an AB pattern for the ZrCH$_2$ unit. This spectrum shows that the molecular symmetry is C_1, the two MeBr$_2$Ox$^-$ ligands are inequivalent, and the sides of the Zr(η^2-CH$_2$Ph) phenyl ring are inequivalent. The low-temperature (−85 °C) ^{19}F and ^{13}C NMR spectra of **23a** show no evidence for B(C$_6$F$_5$)$_4^-$ or CD$_2$Cl$_2$ coordination, although the latter is expected to be difficult to

(47) The model species (MeBr$_2$Ox)$_2$Zr(Me)$^+$ was constructed from the structure of **23a** by replacing the phenyl group of the benzyl ligand with a hydrogen.

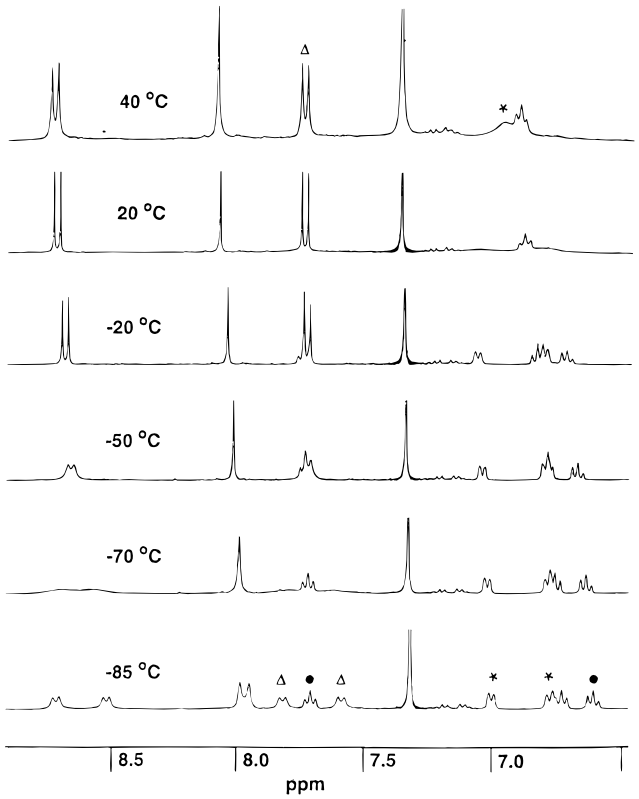

Figure 7. Variable-temperature NMR spectra of [($MeBr_2Ox)_2Zr(\eta^2$-$CH_2Ph)][B(C_6F_5)_4]$ (**23a**). The aromatic region is shown. Assignments at −85 °C are as follows: δ 8.7 (H4), 8.5 (H4), 8.0 (H6), 7.95 (H6), 7.8 (H3, Δ), 7.7 (*m*-Ph, ●), 7.6 (H3, △), 7.0 (*o*-Ph, *), 6.8 (*o*-Ph, *), 6.7 (*p*-Ph), 6.6 (*m*-Ph, ●). The signals at δ 7.32 and 7.06−7.25 are due to benzene and toluene respectively.

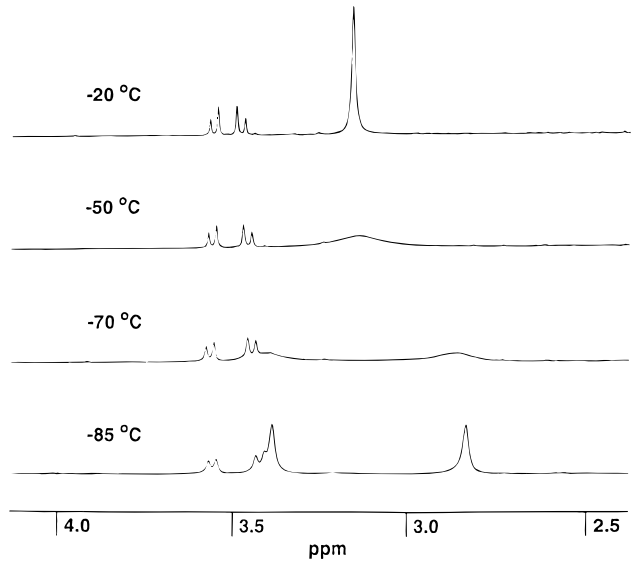

Figure 8. Variable-temperature NMR spectra of [($MeBr_2Ox)_2Zr(\eta^2$-$CH_2Ph)][B(C_6F_5)_4]$ (**23a**). The aliphatic region is shown. In the −85 °C spectrum, the AB pattern centered at δ 3.5 is due to the diastereotopic $ZrCH_2$ hydrogens and the singlets at δ 3.4 and 2.8 are due to the *Me*Br_2Ox hydrogens.

detect.[48] These observations imply that **23a** retains its solid state structure and is rigid on the NMR time scale at −85 °C in CD_2Cl_2 solution.

(48) Fernandez, J. M.; Gladysz, J. A. *Organometallics* **1989**, *8*, 207.

Scheme 2

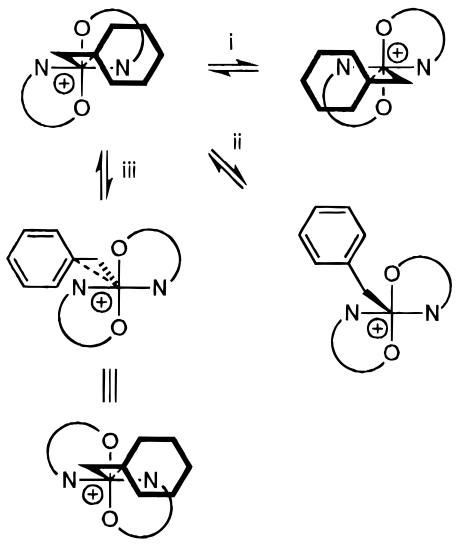

As the sample temperature is raised from −85 °C, two dynamic processes can be detected for **23a**; these are illustrated schematically in Scheme 2. The lower energy process (process i) causes the $MeBr_2Ox^-$ resonances to broaden and ultimately coalesce by ca. −60 °C, but does not perturb the $Zr(\eta^2$-$CH_2Ph)$ resonances (see Figures 7 and 8). This process is identified as rotation of the benzyl ligand around the Zr−C bond (and between two equivalent sites) without cleavage of the η^2-interaction which, as shown in Scheme 2, renders the $MeBr_2Ox^-$ ligands equivalent but not the sides of the Ph ring or the $ZrCH_2$ hydrogens. Above −20 °C, a second, higher energy process (ii) is detected which results in broadening of the *o*-Ph and *m*-Ph resonances of the $ZrCH_2Ph$ group (see Figure 7). The *o*-Ph resonances coalesce at 27 °C, while the *m*-Ph resonances are still broadened into the base line at 40 °C, the highest temperature studied. This higher energy process is identified as rotation around the $ZrCH_2$−Ph bond, which likely proceeds via isomerization of **23a** to a $Zr(\eta^1$−$CH_2Ph)$ intermediate in which essentially free rotation about the $ZrCH_2$−Ph bond can occur, rendering the sides of the Ph group equivalent. Note that as the η^1-CH_2Ph intermediate can collapse to the η^2-CH_2Ph ground state species by coordination of either face of the Ph ring, the η^2−η^1 isomerization rate is twice the rate of exchange of the *o*-Ph or *m*-Ph hydrogens. The barriers for these processes will be discussed below. At 40 °C, a sharp AB pattern is observed for the $ZrCH_2Ph$ methylene hydrogens, indicating the inversion of the metal configuration (process iii), which results in net exchange of the benzyl ligand between the top and bottom faces of the $(MeBr_2Ox)_2Zr^{2+}$ fragment, is still slow on the NMR time scale at this temperature.

The NMR properties of hafnium benzyl cation **24a** are very similar to those of **23a**. The J_{CH} value (143 Hz) for the $HfCH_2$ group establishes that the η^2-benzyl interaction is maintained in solution. The −90 °C ^1H NMR spectrum contains two broad methyl signals, a single set of broad aryl resonances for the $MeBr_2Ox^-$ ligands, and two sharp sets of *o*-Ph and *m*-Ph signals, a *p*-Ph resonance, and a $HfCH_2$ AB pattern for the benzyl ligand. This spectrum is consistent with a C_1-symmetric square pyramidal structure analogous to that observed for **23a** and indicates that the benzyl rotation

process (i) which renders the $MeBr_2Ox^-$ ligands equivalent is not completely frozen out at this temperature. The two *Me*Br_2Ox^- resonances coalesce at −78 °C, and all of the $MeBr_2Ox^-$ resonances are sharp by −30 °C. The $HfCH_2Ph$ *o*-Ph resonances coalesce at −22 °C, and the *m*-Ph resonances coalesce at 10 °C, due to the higher energy $\eta^2-\eta^1$ isomerization process (ii). The room-temperature ^{1}H NMR spectrum of **24a** exhibits an AB pattern for the $HfCH_2$ unit, indicating that as for **23a**, inversion of the metal configuration (process iii) is slow on the NMR time scale at this temperature. This AB pattern broadens significantly above 85 °C (C_6D_5Cl), indicating that inversion of the metal configuration becomes rapid on the NMR time scale in this temperature range. However, sample decomposition also occurs at 85 °C.

Free energy barriers for the dynamic processes i−iii observed for **23a** and **24a** were determined from the ^{1}H NMR line shape changes. The $\Delta G^‡$ (rotation) values for the benzyl group rotation (process i) are very similar for the two compounds (**23a**, 9.8(1) kcal/mol; **24a**, 9.2(2) kcal/mol).[49] The Zr···Ph interaction is not cleaved during this exchange process but switches between the d_{xz} and d_{yz} Zr acceptor orbitals as the Ph is rotated over the Zr−N and Zr−O bonds (see Figure 6). The barrier is probably determined primarily by the difference in energy between these orbitals, which is apparently similar for the two species. In contrast, the $\eta^2-\eta^1$ isomerization barrier $\Delta G^‡$ ($\eta^2-\eta^1$) (process ii) is significantly higher for **23a** (14.0(1) kcal/mol) than for **24a** (11.4(2) kcal/mol).[50] As there should be little steric hindrance to this process, this difference indicates that the M···Ph interaction is stronger in the Zr cation than in the Hf analogue. Interestingly, the barrier estimated for racemization of the five-coordinate cation **24a** (process iii, $\Delta G^‡$ (racemization) > 20(1) kcal/mol) is higher than that determined for the related neutral six-coordinate dibenzyl complex **14a** (17.3(1) kcal/mol).[51,52] A reasonable explanation for this difference is that the rate-limiting step for both racemization processes is dissociation of the nitrogen end of the $MeBr_2Ox^-$ ligand, which would be disfavored in the five-coordinate cation.

Solution Structure and Dynamics of $(MeOx)_2M(R)^+$ Complexes. The variable-temperature NMR properties of the $(MeOx)_2M(R)^+$ cations are quite different from those of the brominated analogues **23a** and **24a** discussed above. The room-temperature ^{1}H NMR spectrum of $(MeOx)_2Zr(CH_2Ph)^+$ (**20a**) contains two sets of $MeOx^-$ resonances, an AB pattern for the $ZrCH_2$ unit, and a single set of $ZrCH_2$*Ph* resonances. As the temperature is lowered, the $MeOx^-$ resonances remain sharp but the $ZrCH_2$*Ph* resonances broaden; in particular, the *o*-Ph and *m*-Ph resonances broaden significantly below −50 °C and are broadened into the base line at −85 °C, the lowest temperature at which spectra were recorded.[53] The J_{HH} (9.6 Hz) and J_{CH} (132 Hz) values for **20a** indicate that the benzyl ligand in this species has some η^2 character but is less distorted than the benzyl ligand in **23a**. The room-temperature ^{1}H NMR spectrum of $(MeOx)_2Hf(CH_2Ph)^+$ (**22a**) is similar to that of **20a** and contains two sets of $MeOx^-$ resonances and one set of $HfCH_2Ph$ resonances. However, the $HfCH_2Ph$ J_{HH} (11.3 Hz) and J_{CH} (125 Hz) values indicate that the benzyl ligand is not significantly distorted. These NMR data for **20a** and **22a** are inconsistent with the square pyramidal structure and the dynamic processes observed for **23a** and **24a** (Scheme 2) because (i) it is very unlikely that the $\eta^2-\eta^1$ isomerization (which, following rotation around the MCH_2-Ph bond, exchanges the sides of the MCH_2*Ph* group) would be faster than rotation about the $Zr-CH_2Ph$ bond (which exchanges the $MeOx^-$ ligands) and (ii) in any case, the Hf···Ph interaction in **22a** is clearly too weak to lock the benzyl ligand in a conformation which results in inequivalent $MeOx^-$ ligands at room temperature.

The room-temperature NMR spectrum of the neopentyl complex $(MeOx)_2Zr(CH_2CMe_3)^+$ (**20b**) is similar to those of **20a** and **22a** and indicates that this species has a C_1 symmetric structure with inequivalent $MeOx^-$ ligands. The $J_{CH}(ZrCH_2)$ value (100 Hz) of **20b** suggests the existence of a Zr−H−Cα agostic interaction in this cation, although this issue was not probed in detail.[37,54] However, α-agostic interactions in related systems are normally very weak, so it is unlikely that the inequivalence of the $MeOx^-$ ligands in this species results from locking of the neopentyl ligand in a particular conformation by a Zr−H−Cα interaction.

Thus, the NMR properties of **20a**, **20b**, and **22a** are not easily rationalized in terms of square pyramidal structures similar to those of **23a** and **24a**, in which a nonclassical bonding interaction locks the apical hydrocarbyl ligand in a particular orientation relative to the Ox^- ligands. Low-temperature ^{19}F NMR (**22a**) and ^{13}C NMR (**20a, 20b, 22a**) spectra show no evidence for the existence of strong interactions between these cations and the $B(C_6F_5)_4^-$ counterion or the CD_2Cl_2 solvent. It thus appears that the structures of the $(MeOx)_2M(R)^+$

(49) Barriers for the benzyl rotation process (i) were calculated from the coalescence of the *Me*Br_2Ox^- resonances and/or H4 resonances using the standard formulae for a two−site, equal population exchange process; i.e., T_c = coalescence temperature; k_c = exchange rate constant at T_c = (2.22)($\Delta\nu$); $\Delta G^‡ = 4.576T_c(10.32 + \log(T_c/k_c))$. For **23a**: Me coalescence $\Delta\nu$(Me) = 199.7 Hz, k_c = 444 s^{-1}, T_c = 215(2) K, $\Delta G^‡$ (rotation) = 9.8(1) kcal/mol; H4 coalescence $\Delta\nu$(H4) = 70.8 Hz, k_c = 158 s^{-1}, T_c = 205(2) K, $\Delta G^‡$ (rotation) = 9.8(1) kcal/mol. For **24a**: Me coalescence $\Delta\nu$(Me) = 176 Hz, k_c = 391 s^{-1}, T_c = 195(3) K, $\Delta G^‡$ (rotation) = 9.2(2) kcal/mol. The H4 resonances of **24a** are not resolved at 188 K, the lowest temperature at which spectra could be obtained.

(50) Barriers for the exchange of the *o*-Ph hydrogens, $\Delta G^‡$ (*o*-Ph exchange), were calculated from the coalescence of the *o*-Ph resonances. Barriers for $\eta^2-\eta^1$ isomerization $\Delta G^‡$ ($\eta^2-\eta^1$) were calculated by assuming that $k(\eta^2-\eta^1) = 2k$(*o*-Ph exchange). For **23a**: $\Delta\nu$(*o*-Ph) = 96 Hz, k_c = 213 s^{-1}, T_c = 300(2) K, $\Delta G^‡$ (*o*-Ph exchange) = 14.2(1) kcal/mol. For **24a**: $\Delta\nu$(*o*-Ph) = 155 Hz, k_c = 344 s^{-1}, T_c = 251(2) K, $\Delta G^‡$ (*o*-Ph exchange) = 11.7(2) kcal/mol.

(51) Estimates for the racemization barrier for **24a** based on line broadening of the $HfCH_2$ AB pattern at 373 K ($\Delta G^‡$ (racemization) ca. 20.8 kcal/mol) and 383 K ($\Delta G^‡$ (racemization) ca. 20.9 kcal/mol) and comparison of experimental and simulated spectra (DNMR5, $\Delta G^‡$ (racemization) ca. 20.7 kcal/mol) are in the range of 21 kcal/mol.

(52) The racemization barrier for **23a** could not be determined because $\Delta\nu$ for the $ZrCH_2$ AB pattern changes significantly with temperature and is very small above 25 °C.

(53) Solubility limitations precluded experiments at lower temperatures, so $\Delta G^‡$ (*o*-Ph exchange) and $\Delta G^‡$ (*m*-Ph exchange) values could not be determined.

(54) (a) Grubbs, R. H.; Coates, G. W. *Acc. Chem. Res.* **1996**, *29*, 85. (b) McGrady, G. S.; Downs, A. J.; Hambin, J. M.; McKean, D. C. *Organometallics* **1995**, *14*, 3783. (c) Leclerc, M. K.; Brintzinger, H. H. *J. Am. Chem. Soc.* **1995**, *117*, 1651. (d) Barta, N. S.; Kirk, B. A.; Stille, J. R. *J. Am. Chem. Soc.* **1994**, *116*, 8912. (e) Etienne, M.; Biasotto, F.; Mathieu, R. *J. Chem. Soc., Chem. Commun.* **1994**, 1661. (f) Etienne, M. *Organometallics* **1994**, *13*, 410. (g) Mashima, K.; Nakamura, A. *J. Organomet. Chem.* **1992**, *428*, 49. (h) Krauledat, H.; Brintzinger, H. H. *Angew. Chem., Int. Ed. Engl.* **1990**, *29*, 1412. (i) Piers, W. E.; Bercaw, J. E. *J. Am. Chem. Soc.* **1990**, *112*, 9406. (j) Brookhart, M.; Green, M. L. H.; Wong, L. L. *Prog. Inorg. Chem.* **1986**, *36*, 1. (k) Dawoodi, Z.; Green, M. L. H.; Mtetwa, V. S. B.; Prout, K.; Schultz, A. J.; Williams, J. M.; Koetzle, T. F. *J. Chem. Soc., Dalton trans.* **1986**, 1629.

Chart 3

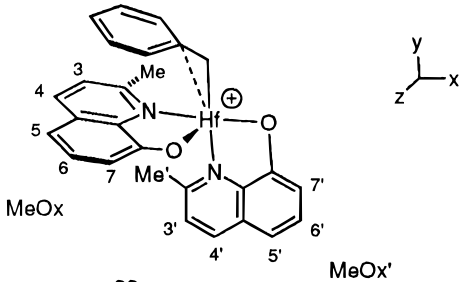

22a

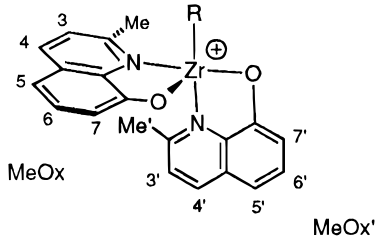

20a R = CH_2Ph
20b R = CH_2CMe_3

cations **20a**,**b** and **22a** are fundamentally different from those of $(MeBr_2Ox)_2M(R)^+$ cations **23a** and **24a**.

To better understand the solution structures of these $(MeOx)_2MR^+$ complexes, we investigated the structure of **22a** in more detail. A complete assignment of the ^1H NMR spectrum, including resonances for the two inequivalent $MeOx^-$ ligands (labeled MeOx and MeOX′ in Chart 3) and the benzyl group was developed based on room-temperature 2-D COSY and NOESY experiments, and geometric information was obtained from the 2-D NOESY spectrum. Two key observations provide important information about the structure of **22a**. (i) NOESY correlations are observed between the *o*-Ph (benzyl) and Me hydrogens, the *m*-Ph (benzyl) and Me hydrogens, and H7 and one of the $HfCH_2$ hydrogens. These correlations establish that the MeOx ligand is spatially close to the CH_2Ph ligand. However, no NOESY correlations are observed between the MeOx′ hydrogens and the $HfCH_2Ph$ hydrogens. (ii) The Me′ resonance ($\delta = 0.59$) is shifted ca. 2 ppm upfield from the range normally observed for $(MeOx)_2MX_2$ complexes. This unusual effect could be due to anisotropic shielding by the $HfCH_2Ph$ phenyl group. However, as noted above, NOESY correlations between the Me′ and $HfCH_2$-Ph hydrogens are not observed. Moreover, a similar high-field Me resonance is observed for $(MeOx)_2Zr(CH_2CMe_3)^+$ (**20b**), which does not contain a benzyl ligand. Therefore, the high-field shift of the Me′ resonance for **22a** (and **20b**) must result from anisotropic shielding by the MeOx ligand; i.e., the Me′ group lies within the shielding region of the MeOx ligand. On the basis of these observations, we propose that **22a** adopts the structure shown in Chart 3, which may be described as a distorted square pyramid with the $MeOx^-$ oxygen in the apical position and a *cis* arrangement of basal nitrogen ligands. Alternatively, this structure may be described as a distorted trigonal bipyramid with apical benzyl and quinolinolato nitrogen ligands. Cations **20a** and **20b** are assigned analogous structures on the basis of the similarity of their NMR spectra to the spectra of **22a**; in particular, both **20a** and **20b** exhibit one high-field and one normal *Me*Ox resonance, which indicates that the arrangement of MeOx ligands is similar to that for **22a**.

Chart 4

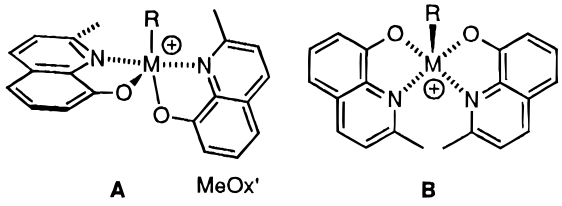

A **B**

The proposed structure for **22a** accommodates the variable-temperature NMR results. The inequivalence of the two quinolinolato ligands results from their geometric relationship, not from a fixed orientation of the hydrocarbyl ligand. Therefore, neither rotation around the $Hf-CH_2Ph$ bond nor $\eta^2-\eta^1$ benzyl isomerization render the MeOx and MeOx′ ligands equivalent.

The proposed structure for $(MeOx)_2M(R)^+$ complexes is formally related to the structure of the neutral $(MeOx)_2MR_2$ precursors, as shown in eq 13. Alkyl

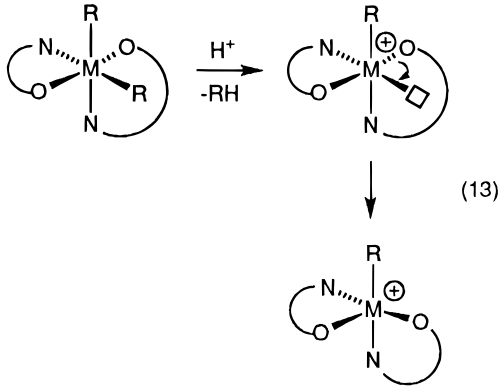

(13)

abstraction yields a five-coordinate species, which can relax to the proposed structure by a shift of one of the $MeOx^-$ oxygen donors.

The structural difference between the $(MeBr_2Ox)_2MR^+$ (**23a**, **24a**) and $(MeOx)_2MR^+$ (**20a**, **20b**, **22a**) cations may be rationalized in terms of electronic effects. As noted above, the $(MeBr_2Ox)_2M(CH_2Ph)^+$ cations **23a** and **24a** adopt square pyramidal structures with an apical-benzyl, *trans*-O, *trans*-N ligand arrangement. A key feature of this structure is that the potential π-donor phenoxides must share a single metal π-acceptor orbital (d_{yz}, Figure 6). This structure is disfavored for $(MeOx)_2M(R)^+$ species **20a**, **20b**, and **22a** because the oxygens in the $MeOx^-$ ligand are stronger π-donors than those in the $MeBr_2Ox^-$ ligand. In the proposed apical-O, *cis*-N structure in Chart 3, the two quinolinolato oxygens do not compete for the same metal d acceptor orbital; i.e., the apical oxygen can form a $O-Zr$ π-bond with the d_{yz} orbital, and the basal oxygen can form an $O-Zr$ π-bond with the d_{xz} orbital (using the coordinate system in Chart 3).

Alternative Structural Possibilities for $(MeOx)_2M(R)^+$ Complexes. Two other possible structures (**A** and **B** in Chart 4) were considered for **20a**,**b** and **22a** but were ruled out on the basis of NMR observations. Structure **A**, in which the MeOx′ ligand is oriented in a different manner than that in the proposed structures of **20a**,**b** and **22a**, is inconsistent with the observation

Chart 5[a]

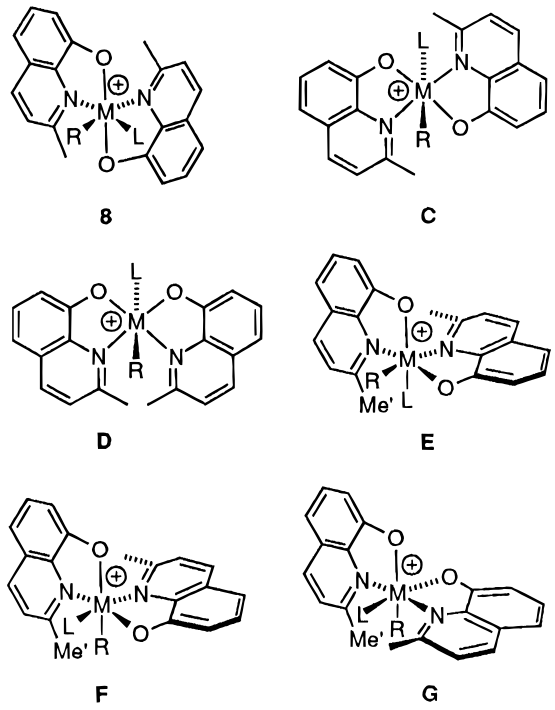

[a] 5,7 Ox substituents omitted.

of NOESY correlations between the benzyl ligand and only one of the $MeOx^-$ ligands and does not provide a rationale for the high-field shift of one of the Me resonances. This structure is disfavored because the two quinolinolato oxygens compete for the same metal d orbital for O−M π-donation and because the strong *trans*-influence hydrocarbyl and MeOx′ oxygen ligands are in a *trans* orientation. Structure **B**, which is the *cis* isomer of the structures of **23a** and **24a**, contains two equivalent $MeOx^-$ ligands and is thus inconsistent with the C_1 symmetry of these complexes implied by the NMR data. Inspection of models suggests that this structure is disfavored by unfavorable steric interactions between the two $MeOx^-$ methyl groups. However, displacement of one $MeOx^-$ pyridine to a position *trans* to the benzyl group in **B** would relieve Me/Me steric interactions and result in the structures proposed in Chart 3.[55]

Synthesis and Characterization of $[(MeBr_2Ox)_2M(CH_2Ph)(PMe_3)][B(C_6F_5)_4]$ Complexes. The six possible isomers of a $(Ox)_2M(R)(L)^+$ complex (**8** and **C**−**G**) are illustrated in Chart 5. As noted in the introduction, a key consideration in the choice of the $(Ox)_2M(R)^+$ system for the development of new electrophilic metal alkyl reagents/catalysts was the expectation that these species would coordinate ligands or potential substrates in a position *cis* to the hydrocarbyl ligand; i.e., that $(Ox)_2M(R)(L)^+$ species would adopt structures of type **8** which are analogous to the structures of $(Ox)_2MR_2$ compounds. A *cis* relationship of the R and substrate groups is necessary for subsequent insertion or σ-bond metathesis reactions.

The C_1 symmetry of the amine complex $(MeBr_2Ox)_2Zr(CH_2Ph)(NMe_2Ph)^+$ (**21a**) (as determined by NMR spectroscopy) implies that the amine and benzyl ligand are *cis* because the possible *trans* structures **C** and **D** have C_2 and C_s symmetry, assuming free rotation about the Zr−amine and Zr−C bonds. However, the data for **21a** do not establish the orientations of the $MeBr_2Ox^-$ ligands, and due to overlap among the NMe_2*Ph* and CH_2*Ph* resonances, details about the orientation and dynamics of the benzyl ligands are unknown.

To further probe the structures of $(Ox)_2M(R)(L)^+$ species, the more stable PMe_3 adducts **25a** and **26a** were prepared (eq 14). The ^{1}H NMR spectra of **25a** and **26a**

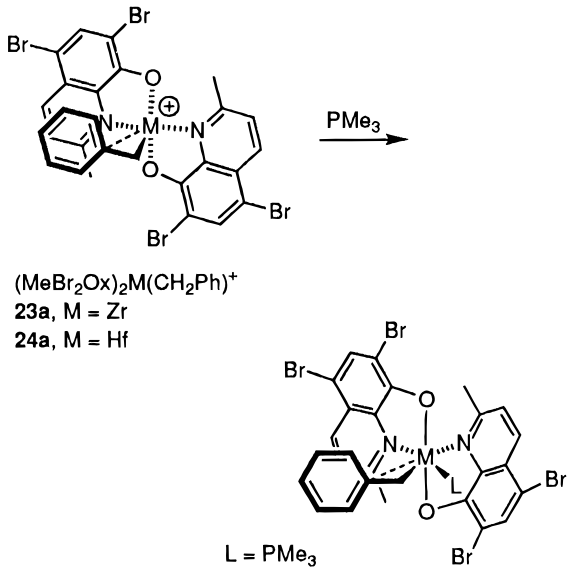

(14)

establish that both cations contain 1 equiv of PMe_3 and that PMe_3 exchange is slow on the NMR time scale at room temperature.

The ^{1}H NMR spectrum of **25a** is unchanged over the temperature range from −80 to 25 °C and establishes that this species has C_1 symmetry. This conclusion is confirmed by the ^{13}C NMR spectrum. The ^{1}H spectrum contains two sets of $MeBr_2Ox^-$ resonances, showing that the two ligands are inequivalent, and two sets of *m*-Ph and *o*-Ph $ZrCH_2Ph$ resonances, indicating that the sides of the benzyl phenyl ring are inequivalent. All of the ^{1}H NMR resonances were assigned by 2-D COSY and NOESY spectroscopy (−80 °C). The $ZrCH_2$ J_{HH} (7.5 Hz) and J_{CH} (145 Hz) values establish that the benzyl ligand is coordinated in an η^2 mode, and the fact that the sides of the benzyl phenyl ring are inequivalent indicates that the η^2−η^1 exchange is slow on the NMR time scale. For d^0 group 4 metal phosphine alkyl complexes, J_{PH} values (P−M−CH) are similar for both *cis* and *trans* structures (0−14 Hz) while J_{PC} values (P−M−CH) are small for *cis* structures (<5 Hz) but much larger for *trans* structures (>30 Hz).[56,57] The J_{PH} (9.4, 5.0 Hz) and J_{PC} (9 Hz) values for **25a** are, thus, most consistent with a structure in which the benzyl and PMe_3 ligands are *cis*.

(55) The apical-R, *trans*-O, *trans*-N square pyramidal structure may be less sterically congested than structures **A** or **B** and is, thus, favored for $(MeBr_2Ox)_2M(R)^+$ species in which O−Zr π−bonding is not important.

(56) Representative J_{PH} and J_{PC} (P−M−CH) values group 4 metal complexes (a). $TiCl_3$(dmpe)Me: J_{PH}(*cis*) = J_{PH}(*trans*) = 7.7 Hz, J_{PC}(*cis*) not observed, J_{PC}(*trans*) = 32.4 Hz. $TiCl_3$(dmpe)Et: J_{PH}(*cis*), J_{PH}(*trans*) = 12.0 Hz and unresolved, J_{PC}(*cis*) = 3.1 Hz, J_{PC}(*trans*) = 31.8 Hz. See ref 54k. (b) $Zr(CH_2SiMe_2NSiMe_3)_2$(dmpe): J_{PH}(*cis*) = 3.2, 3.2 Hz, J_{PC}(*cis*) = "on the order of the natural line width." Planalp, R. P.; Andersen, R. A. *Organometallics* **1983**, *2*, 1675. (c) $TiMe_2(CH_2CH_2)$-(η^2-dmpe)(η^1-dmpe): J_{PH}(*cis*) = 4.5 Hz, J_{PC}(*cis*) not observed. Spencer, M. D.; Morse, P. M.; Wilson, S. R.; Girolami, G. S. *J. Am. Chem. Soc.* **1993**, *115*, 2057.

Table 3. Ethylene Polymerization Data[a]

entry	catalyst	μmol of catalyst	cocatalyst[b]	μmol of cocatalyst	solvent (mL)	time (h)	temp (°C)	yield (g)	activity (kg/mol·atm·h)
1[c,d]	$(MeOx)_2Zr(CH_2Ph)_2$ (**9a**)	32	$HNMe_2Ph^+$	31	1/1 C_6H_5Cl/toluene (20)	0.5	23	0.0	
2[c]	$(MeOx)_2Zr(CH_2CMe_3)_2$ (**9b**)	33		29		0.5	23	0.0	
3[e]	$(MeBr_2Ox)_2Zr(CH_2Ph)_2$ (**11a**)	17		17		0.5	23	0.49(7)	19(3)
4[e]		17	$HMePh_2^+$	17		0.5	23	0.69(1)	28(1)
5[e]		17		17		0.5	60	0.57(3)	22(1)
6[c]		16		17		0.5	23	0.41	26[f]
7[c]		17		16	toluene (20)	0.5	23	0.19	12
8[c]		17		16	C_6H_5Cl (20)	0.5	23	0.1	6.2
9[e]	$(MeBr_2Ox)_2Hf(CH_2Ph)_2$ (**14a**)	17	$HNMe_2Ph^+$	17	1/1 C_6H_5Cl/toluene (20)	0.5	23	0.05(1)	1.9(5)
10[e]		17	$HNMePh_2^+$	17		0.5	23	0.18(1)	6.8(3)
11[e]		17		17		0.5	60	0.57(5)	22(3)
12[g]	$(MeBr_2Ox)_2Zr(CH_2Ph)_2$ (**11a**)	44	$HNMe_2Ph^+$	44	toluene (500)	1.0	30	3.2	9.1[h]
13[g]		44	$B(C_6F_5)_3$	44		1.0	30	1.5	4.2[i]
14[j]	$(MeBr_2Ox)_2ZrCl_2$ (**16**)	44	MAO	30000		1.0	30	0.67	1.9[k]
15[g]		44	$HNMe_2Ph^+$	44		1.0	30	14.6	41[l]

[a] Yields and activities for entries 3−5 and 9−11 are averages of 2−4 experiments. [b] Anion of HNR_3^+ cocatalysis is $B(C_6F_5)_4^-$. [c] Catalyst and cocatalyst were mixed in the solvent (10 min) and then charged with 2 atm of ethylene. [d] Similar results (i.e., no activity) were obtained in pure C_6H_5Cl solution at 23 and 55 °C. [e] Catalyst and cocatalyst were mixed in the solvent (10 min) and then charged with 3 atm of ethylene. [f] $M_n = 576$, $M_w/M_n = 1.18$. [g] TIBA (750 μmol, Al/Zr = 17) added. Ethylene pressure = 8 atm. [h] $M_n = 2.11 \times 10^4$, $M_w/M_n = 16.3$. [i] $M_n = 4.8 \times 10^4$, $M_w/M_n = 13.9$. [j] Ethylene pressure = 8 atm. [k] $M_w = 4.6 \times 10^5$ (light scattering). [l] $M_w > 2 \times 10^6$ (light scattering).

Four isomers with *cis* benzyl and PMe_3 groups are possible for $(Ox)_2M(CH_2Ph)(PMe_3)^+$ species: the *trans*-O, *cis*-N structure **25a** shown in eq 14 (i.e., a type **8** structure) and **E**−**G** in Chart 5 which differ in the arrangement of N and O ligands. The 2-D NOESY spectrum for **25a** shows a strong correlation between a *m*-Ph resonance and a *Me*Br_2Ox^- resonance, indicating that the benzyl Ph ring points toward a $MeBr_2Ox^-$ ligand and away from the PMe_3 group. No other interligand correlations are observed. Additionally, both *Me*Br_2Ox^- resonances appear in the normal range (δ 2.25, 2.02). These observations are consistent with the structure **25a** (eq 14; identical to **8**, Chart 5) but are inconsistent with structures **E**−**G**. In **E** and **F**, one Ox methyl group lies within the shielding region of the other Ox^- ligand (that containing Me′) so that one Me resonance should appear at high field, as observed for **20a**, **20b**, and **22a**. For **F** and **G**, a $ZrCH_2$/Me′ NOESY correlation is expected since these groups are forced close together in the expected most stable conformation. Therefore, it is concluded that **25a** adopts the *trans*-O, *cis*-N structure shown in eq 14.

The ^{1}H NMR spectrum of $(MeBr_2Ox)_2Hf(\eta^2\text{-}CH_2Ph)(PMe_3)^+$ (**26a**) is similar to that of **25a** below −30 °C. Above this temperature, however, the two *o*-Ph resonances and the two *m*-Ph resonances for the benzyl phenyl group broaden, ultimately coalescing at 25 and 30 °C, respectively. The resonances for the two inequivalent $MeBr_2Ox^-$ ligands do not broaden up to 40 °C, the highest temperature investigated. The $HfCH_2$-Ph J_{PC} value (4 Hz) indicates that the PMe_3 and benzyl ligands are *cis*. These data are consistent with a C_1-symmetric *cis* structure analogous to that for **25a**; however, the η^2-benzyl interaction is weaker in **26a** than in **25a** and $\eta^2-\eta^1$ isomerization, which leads to equivalencing of the sides of the Ph group via rotation around the MCH_2-Ph bond in the η^1-benzyl intermediate, is more rapid. The barrier calculated for exchange of the sides of the benzyl phenyl group is $\Delta G^\ddagger$ (*o*-Ph exchange) = 13.8(1) kcal/mol.[58] Surprisingly, this barrier is higher than that calculated for the same process in the analogous base-free cation **24a** (11.7(2) kcal/mol). As the Hf···Ph interaction is expected to be stronger in base-free **24a** than in PMe_3 adduct **26a**, the higher barrier in the latter species probably results from steric crowding between the benzyl and PMe_3 ligands, which restricts the mobility of the benzyl group.

Recently, Floriani showed that (hydroxyphenyloxazolinato)$_2$M$(CH_2Ph)_2$ and (hydroxyphenyloxazolinato)$_2$Hf$(CH_2Ph)(THF)^+$ (M = Zr, Hf) adopt structures analogous to those observed here for $(Ox)_2M(CH_2Ph)_2$ and $(Ox)_2M(CH_2Ph)(L)^+$ species.[6]

Olefin Polymerization Studies. The foregoing sections describe the synthesis and structures of a new class of d^0 metal alkyl cations which incorporate the key features believed to be required for olefin polymerization and other "electrophilic metal alkyl" reactivity. Accordingly, we have investigated the ethylene polymerization reactivity of selected $(MeOx)_2Zr(R)^+$ (**20a**, R = CH_2Ph; **20b**, R = CH_2CMe_3) and $(MeBr_2Ox)_2M(CH_2Ph)^+$ (**23a**, M = Zr; **24a**; M = Hf) complexes. These cationic species were generated *in situ* from the appropriate $(Ox)_2MR_2$ precursors via the protonolysis reactions in eq 9 (**20a**,**b**) or eq 11 (**23a**, **24a**) and their ethylene polymerization behavior compared under similar conditions (toluene/chlorobenzene 1/1 by volume, 23 °C, 2−3 atm, 30 min polymerization time). As summarized in Table 3, at 23 °C under these conditions the ethylene polymerization activity order is **23a** > **24a** >> **20a**,**b** (not active) i.e., only the cations containing $MeBr_2Ox^-$ ligands are active (compare entries 1, 2, 4, 10). When the polymerization temperature is raised to 60 °C, the activity of **23a** decreases (entry 5) and that of **24a** increases (entry 11), such that these catalysts exhibit comparable activities at this temperature.

Exposure of a solution of **23a** to 2 atm of ethylene at 23 °C (entry 6) results in a visibly exothermic reaction,

(57) For a review on early metal phosphine complexes, see: Fryzuk, M. D.; Haddad, T. S.; Berg, D. J.; Rettig, S. J. *Pure Appl. Chem.* **1991**, *63*, 845.

(58) Barriers for the exchange of the *o*-Ph hydrogens $\Delta G^\ddagger$ (*o*-Ph exchange) and the *m*-Ph hydrogens $\Delta G^\ddagger$ (*m*-Ph exchange) were calculated from the coalesence of the *o*-Ph resonances and of the *m*-Ph resonances and are identical as expected. For *o*-Ph exchange: $\Delta\nu$(*o*-Ph) = 343 Hz, $k_c = 761$ s^{-1}, $T_c = 303(2)$ K, $\Delta G^\ddagger$ (*o*-Ph exchange) = 13.8(1) kcal/mol. For *m*-Ph exchange: $\Delta\nu$(*m*-Ph) = 455 Hz, $k_c = 1010$ s^{-1}, $T_c = 308(2)$ K, $\Delta G^\ddagger$ (*m*-Ph exchange) = 13.8(1) kcal/mol. The apparent barrier for $\eta^2-\eta^1$ isomerization is calculated by assuming that $k_{(\eta^2-\eta^1)} = 2k$(*o*-Ph exchange) is $\Delta G^\ddagger$ ($\eta^2-\eta^1$) = 13.3(1) kcal/mol.

immediate formation of solid polymer, and rapid (ca. 10 min) darkening of the reaction mixture from yellow to brown. These observations suggest that polymerization is initially rapid but that rapid catalyst deactivation also occurs; the activity based on a 30 min polymerization time is therefore a lower limit. The polymer produced by **23a** under these conditions is a linear, low molecular weight polyethylene (0.3 branches/chain; $M_n = 576$) and has a very narrow polydispersity ($M_w/M_n = 1.18$) characteristic of a single site catalyst.[59] NMR analysis shows the presence of vinyl (50%) and saturated end groups (50%), consistent with chain transfer via β-H elimination, i.e., the polymer is a C_{44} α-olefin. It is reasonable to propose that chain growth occurs on intact $(MeBr_2Ox)_2Zr(R)^+$ cations; however, as yet there is no direct evidence regarding this point.[60] Catalyst deactivation may occur via a variety of processes, including migration of the growing alkyl chain or a hydride (following β-H elimination) from Zr to a $MeBr_2Ox^-$ ligand, as observed for $(MeBr_2Ox)_2Zr(CH_2Ph)_2$.

The activity of **23a** is lower in chlorobenzene (entry 8) or toluene (entry 7) than in the mixed toluene/chlorobenzene (1/1) solvent (entry 6). Visual observations (darkening of reaction mixture) suggest that catalyst deactivation is faster in chlorobenzene which may reduce the observed activity. Differences in ion pairing in toluene versus chlorinated solvents are also expected to influence activity.

The activity of the amine complex $(MeBr_2Ox)_2Zr(CH_2Ph)(NMe_2Ph)^+$ (**21a**) (generated *in situ* by the reaction of **11a** with $[HNMe_2Ph][B(C_6F_5)_4]$; eq 10) is somewhat lower than that of **23a** (entry 3 vs 4), possibly as a result of reversible coordination of NMe_2Ph. Similarly, $(MeBr_2Ox)_2Hf(CH_2Ph)(NMe_2Ph)^+$ is less active than **24a** (entry 9 vs 10). Aluminum cocatalysts (added as scavengers) have a significant effect on the ethylene polymerization performance of **21a**. The addition of $Al(^iBu)_3$ (17 equiv vs Zr) to **21a** (entry 12) results in a significant increase in the polymer molecular weight ($M_n = 21\,100$) and broadening of the molecular weight distribution ($M_w/M_n = 16.3$). Similar results are obtained when $(MeBr_2Ox)_2Zr(CH_2Ph)_2$ is activated by $B(C_6F_5)_3$ in the presence of $Al(^iBu)_3$ (entry 13). The broad molecular weight distributions indicate that these systems are multisite catalysts. It is likely that the added AlR_3 reagent abstracts a $MeBr_2Ox^-$ ligand from either **11a** or **21a** or $(MeBr_2Ox)_2Zr(R)^+$ species (R = growing chain), resulting in complex secondary chemistry and generation of more than one active catalyst. As noted above, $MeBr_2Ox^-$ transfer to Al is observed in the reactions of $AlMe_3$ with $(MeBr_2Ox)_4Zr$ (**13**), $(MeBr_2Ox)_2ZrCl_2$ (**16**), and $(MeBr_2Ox)_2Zr(NMe_2)_2$ (**17**).

The activation of the dichloride complex $(MeBr_2Ox)_2ZrCl_2$ (**16**) for ethylene polymerization was also briefly investigated. Complex **16** is activated by methylalumoxane (MAO, Al/Zr = 680, run 14) or by treatment with $Al(^iBu)_3$ followed by $[HNMe_2Ph][B(C_6F_5)_4]$ (run 15). In each case, moderate activity, similar to that observed for **23a**, is observed. However, the polymer molecular weight is much higher, ranging from $M_w = 460\,000$ (light scattering) for the MAO cocatalyst to >2 000 000 for the $[HNR_3][B(C_6F_5)_4]$ experiments. GPC measurements were precluded by the low solubility of these materials, so polydispersity data are not available. The origin of this increase in molecular weight is unclear at present, however, it is likely that $MeBr_2Ox^-$ ligand transfer to Al occurs in the catalyst generation process, leading to complex chemistry.

Conclusions

New Zr(IV) and Hf(IV) alkyl complexes containing substituted 8-quinolinolato ancillary ligands have been prepared and structurally characterized by X-ray diffraction and NMR spectroscopy. Neutral bis(hydrocarbyl) complexes of general type $(Ox)_2MR_2$ adopt C_2-symmetric, distorted octahedral structures with a *trans*-O, *cis*-N, *cis*-R ligand arrangement. Protonolysis of these species with bulky ammonium reagents yields base-free $(Ox)_2M(R)^+$ cations, which can be isolated as the $B(C_6F_5)_4^-$ salts. Cationic $(MeBr_2Ox)_2M(\eta^2\text{-}CH_2Ph)^+$ species **23a** and **24a**, which contain the electron-withdrawing $MeBr_2Ox^-$ ancillary ligand, adopt square pyramidal structures in which the strongly distorted η^2-CH_2Ph group occupies the apical position and the basal $MeBr_2Ox^-$ ligands are arranged in a *trans*-O, *trans*-N fashion. In contrast, distorted square pyramidal structures with an apical-O, *cis*-N ligand arrangement are proposed for $(MeOx)_2M(R)^+$ cations **20a**, **20b**, and **22a**. The electronic properties of the Ox^- ligands and steric interactions within the $(Ox)_2M$ unit influence the structural preferences of these species. In particular, because both Ox^- oxygens must compete for π-donation to the same metal acceptor orbital in the apical-R, *trans*-O, *trans*-N square pyramidal structure observed for **23a** and **24a**, this structure is disfavored for $(MeOx)_2M(R)^+$ species which contain the stronger π-donor $MeOx^-$ ligand. Cations **23a** and **24a** form six-coordinate $(MeBr_2Ox)_2M(\eta^2\text{-}CH_2Ph)(L)^+$ adducts with NMe_2Ph and PMe_3. These species adopt structures analogous to those of neutral $(Ox)_2MR_2$ species, in which the benzyl and L groups are *cis* and the *trans*-O, *cis*-N $(Ox)_2M$ unit has C_2 symmetry. Thus, the $(Ox)_2M$ unit undergoes significant structural change upon conversion of six-coordinate $(Ox)_2M(R)_2$ or $(Ox)_2M(R)(L)^+$ species to five-coordinate $(Ox)_2M(R)^+$ cations.

The neutral $(Ox)_2MR_2$ complexes and the $(Ox)_2MR^+$ cations are both chiral but undergo inversion of configuration at the metal center in solution, most likely by M−N bond cleavage. Interestingly, the inversion barriers are significantly higher for the five-coordinate cations (>20 kcal/mol) than the six-coordinate neutral species (15−18 kcal/mol), which may be explained by the stronger M−N bond strength in the cations.

Several observations provide insight to Lewis acidity trends in $(Ox)_2MR_2$ and $(Ox)_2M(R)^+$ complexes. The $(MeBr_2Ox)_2M(\eta^2\text{-}CH_2Ph)^+$ cations **23a** and **24a** form adducts with NMe_2Ph while the MeOx analogue **20a** does not, indicating that the electron-withdrawing Br substituents increase the Lewis acidity at the metal center as expected. Comparison of the MCH_2Ph J_{HH} and J_{CH} values and $\eta^2-\eta^1$ isomerization barriers ($\Delta G^{\ddagger}$ (η^2-η^1)) for $(Ox)_2M(CH_2Ph)_2$ and $(Ox)_2M(CH_2Ph)^+$ complexes (Table 4) indicates that the M···Ph interactions

(59) The M_w/M_n value may be decreased from the expected value of 2.0 by loss of some soluble low molecular weight material during isolation of the polymer.

(60) Assuming that all $(MeBr_2Ox)_2Zr(CH_2Ph)^+$ centers are activated and initially insert ethylene into the Zr−CH_2Ph bond, the catalyst charge, polymer yield, and polymer M_n values imply that on average each site produces 44 chains and, therefore, that $^1/_{88}$ of the chain ends should be −CH_2Ph groups. This low concentration of end groups is not detectable by NMR.

Table 4. NMR Coupling Constants (MCH_2Ph) and Free Energy Barriers for the $\eta^2-\eta^1$ Benzyl Isomerization of $(Ox)_2M(CH_2Ph)_2$, $(Ox)_2M(CH_2Ph)^+$, and $(Ox)_2M(CH_2Ph)(L)^+$ Complexes

compound	J_{HH} (Hz)	J_{CH} (Hz)	$\Delta G^{\ddagger}$ ($\eta^2-\eta^1$) (kcal/mol)
$(MeOx)_2Zr(CH_2Ph)_2$ (**9a**)	8.5	129	
$(MeOx)_2Hf(CH_2Ph)_2$ (**10a**)	10.2	120	
$(MeOx)_2Zr(CH_2Ph)^+$ (**20a**)	9.6	132	
$(MeOx)_2Hf(CH_2Ph)^+$ (**22a**)	11.3	125	
$(MeBr_2Ox)_2Zr(CH_2Ph)_2$ (**11a**)	8.8	130	
$(MeBr_2Ox)_2Hf(CH_2Ph)_2$ (**14a**)	10.9	122	
$(MeBr_2Ox)_2Zr(CH_2Ph)^+$ (**23a**)	8.8	145	14.0(1)
$(MeBr_2Ox)_2Hf(CH_2Ph)^+$ (**24a**)	10.0	143	11.4(2)
$(MeBr_2Ox)_2Zr(CH_2Ph)(NMe_2Ph)^+$ (**21a**)	9.1		
$(MeBr_2Ox)_2Hf(CH_2Ph)(NMe_2Ph)^+$	11.3		
$(MeBr_2Ox)_2Zr(CH_2Ph)(PMe_3)^+$ (**25a**)	7.5	145	
$(MeBr_2Ox)_2Hf(CH_2Ph)(PMe_3)^+$ (**26a**)	9	141	

are stronger and the benzyl ligands are more distorted in the Zr species than in the corresponding Hf species. This trend suggests that the Zr complexes are stronger Lewis acids than the corresponding Hf complexes. While few quantitative data are available, the relative Lewis acidity of ZrX_4 and HfX_4 complexes varies depending on the nature of the X groups and the Lewis base.[61]

The ethylene polymerization behavior of $(Ox)_2MR^+$ species is strongly influenced by the ligand properties and the identity of the metal. The $(MeBr_2Ox)_2M(\eta^2\text{-}CH_2Ph)^+$ cations **23a** and **24a** exhibit moderate ethylene polymerization activity, while the MeOx analogues $(MeOx)_2Zr(CH_2Ph)^+$ (**20a**) and $(MeOx)_2Zr(CH_2CMe_3)^+$ (**20b**) are inactive, at least under the conditions studied. The enhancement in activity due to incorporation of the electron-withdrawing bromine substituents in **23a** and **24a** may result from the increased metal Lewis acidity, from structural effects (ligand arrangement in square pyramidal $(Ox)_2MR^+$ structures), or other factors. Neither **20a** nor **20b** coordinate NMe_2Ph, so these species are probably not electrophilic enough to coordinate and activate ethylene. In contrast, electron-donating substituents generally increase the olefin polymerization activity of metallocene catalysts.[62]

This work shows that the general catalyst design principles developed for metallocene systems can be extended to $(Ox)_2MR_2/(Ox)_2MR^+$ systems and that electron-withdrawing $MeBr_2Ox^-$ ligands are preferable to $MeOx^-$ ligands for olefin polymerization activity. However, the $(Ox)_2MR^+$ systems differ from Cp_2MR^+ systems in several respects, which has a deleterious effect on catalyst performance. (i) The $(Ox)_2M$ unit undergoes significant structural change when a $(Ox)_2MR_2$ species is converted to a $(Ox)_2MR^+$ cation. This structural relaxation presumably stabilizes and reduces the electrophilicity of the cation and disfavors coordination of an olefin or other Lewis base. In contrast, the Cp_2M structure is not significantly perturbed when a Cp_2MR_2 species is ionized to an active Cp_2MR^+ cation.[1] (ii) The $(Ox)_2MR^+$ cations contain electrophilic sites at the metal center and at the C2 and C4 carbons of the Ox ligands, i.e., the electrophilicity is not concentrated at the metal center as in a $Cp_2M(R)^+$ system. This presumably reduces the electrophilicity of the metal site. Floriani has noted a similar effect in group 4 metal (N_4-macrocycle)MR_2 and (N_4-macrocycle)MR^+ compounds.[4c] (iii) The presence of electrophilic sites (C2 and C4) and nucleophilic sites (Ox^- oxygens) on the Ox^- ligands in $(Ox)_2MR_2$ and $(Ox)_2MR^+$ complexes leads to deleterious reactions including thermal rearrangement via nucleophilic alkyl migration to C2 and Ox^- transfer to Al reagents. (iv) Chiral $(Ox)_2MR_2$ complexes undergo facile inversion of configuration at the metal center. Studies aimed at circumventing these problems by modification of the Ox^- ligands are in progress.

Chart 6

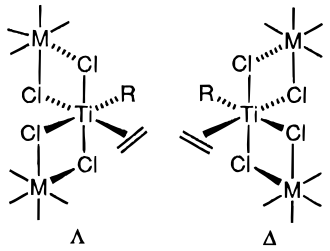

Finally, it may be noted that the $(Ox)_2MR_2$ and $(Ox)_2M(R)^+$ systems studied here bear a topological resemblance to the chiral, octahedral Ti active sites which have been proposed for supported Ziegler–Natta catalysts (Chart 6).[63] Efforts are underway to develop more reactive and stereorigid, octahedral, and five-coordinate $(LL)_2MR_2$ and $(LL)_2MR^+$ species based on bidentate ancillary ligands (LL), which may be of use for modeling the properties and reactivity of such sites and for catalytic applications.

Experimental Section

General Considerations. All experiments were performed under nitrogen or vacuum using a glovebox or a high-vacuum line. Benzene, toluene, pentane, hexanes, ether, and THF were dried by distillation over Na/benzophenone. Methylene chloride and chlorobenzene were distilled over CaH_2. Benzene-d_6, THF-d_8, and toluene-d_8 were dried over Na, and methylene chloride-d_2 and chlorobenzene-d_5 were dried over P_2O_5. NMR spectra were obtained on Bruker AMX-360 (^1H, ^{13}C, ^{11}B) or AC-300 (^{19}F) instruments at ambient probe temperature (25 °C), unless indicated otherwise. J_{CH} values were obtained from gated $\{^1H\}^{13}C$ NMR spectra. ^1H NMR assignments for $(Ox)_2MR_2$ and $(Ox)_2MR^+$ complexes were made by analogy to the assignments for MeOxH and $MeBr_2OxH$[64,65] and were confirmed by homonuclear decoupling experiments for **10a**, **20a**,**b**, and **22a** and COSY and NOESY experiments for **19**, **22a**, and **25a**. NMR assignments are reported using the numbering scheme in Chart 1. For **20a**, **20b**, and **22a**, the entries Hx′ and Me′ and Hx and Me denote the hydrogens in the MeOx′ and MeOx ligands, respectively; see Chart 3.

(61) (a) Felten, J. J.; Anderson, W. P. *J. Organomet. Chem.* **1974**, *82*, 375. (b) Felten, J. J.; Anderson, W. P. *J. Organomet. Chem.* **1972**, *36*, 87. (c) Chung, F. M.; Westland, A. D. *Can. J. Chem.* **1969**, *47*, 195. (d) Krzhizhanovskaya, E. E; Suvarov, A. V. *Zh. Neorg. Khim.* **1971**, *16*, 3380. (e) Hummers, W. S.; Tyree, S. Y., Jr.; Yolles, S. *J. Am. Chem. Soc.* **1952**, *74*, 139.

(62) See discussion in ref 1g and (a) Lee, I.; Gauthier, W. J.; Ball, J. A.; Iyengar, B.; Collins, S. *Organometallics* **1992**, *11*, 2115 and references therein.

(63) See: Corradini, P.; Busico, V.; Cavallo, L.; Guerra, G.; Vacatello, M.; Venditto, V. *J. Mol. Catal.* **1992**, *74*, 433 and references therein.

(64) (a) ^1H NMR data for MeOxH (C_6D_6): δ 8.68 (s, 1H, OH), 7.42 (d, J = 8.4 Hz, 1H, H4), 7.16 (dd, J = 7.6, 1.3 Hz, 1H, H5), 7.11 (t, J = 8.0, 1H, H6), 6.96 (dd, J = 8.1, 1.3 Hz, 1H, H7), 6.63 (d, J = 8.4 Hz, 1H, H3), 2.29 (s, 3H, Me). NOESY results confirm the assignments of H5 and H7. ^1H NMR data for $MeBr_2OxH$ (C_6D_6): δ 8.60 (s, 1H, OH), 7.81 (d, J = 8.6 Hz, 1H, H4), 7.60 (s, 1H, H6), 6.51 (d, J = 8.6 Hz, 1H, H3), 2.12 (s, 3H, Me).

(65) For NMR studies of 8-quinolinols and 8-quinolinolato complexes, see: (a) Baker, H. C.; Sawyer, D. T. Anal. *Chem.* **1968**, *40*, 1945. (b) Hanrahan, E. S.; Chakrabarty, M. R. *J. Magn. Reson.* **1970**, *2*, 19.

Coupling constants are reported in Hertz. Elemental analyses were performed by E & R Microanalytical Laboratory, Inc. The following compounds were prepared by literature methods: MR_4 (M = Zr, R = CH_2Ph, CH_2CMe_3, CH_2SiMe_3; M = Hf, R = CH_2Ph),[66] $[HNMe_2Ph][B(C_6F_5)_4]$, $[HNMePh_2][B(C_6F_5)_4]$.[6a] MeOxH and $MeBr_2OxH$ were obtained from Aldrich and used without purification.

(MeOx)Li (2-Li). A solution of BuLi (32 mmol) in pentane/hexanes (20 mL) was added to a slurry of MeOxH (5.17 g, 32.5 mmol) in pentane (30 mL) at room temperature. An off-white precipitate appeared. The reaction mixture was stirred for 10 min and filtered, yielding an off-white solid (4.80 g, 90.8%). The identity of **2-Li** was confirmed by hydrolysis to MeOxH and by reaction with $ZrCl_4$ to yield $(MeOx)_2ZrCl_2$. ^{1}H NMR (THF-d_8): δ 7.91 (1H, br), 7.09 (2H, br), 6.71 (2H, br), 2.47 (3H, br, Me).

($MeBr_2Ox$)Li (3-Li). A solution of BuLi (27.5 mmol) in toluene (40 mL) was added to a toluene solution (50 mL) of $MeBr_2OxH$ (9.21 g, 29.1 mmol) over 5 min at room temperature. The reaction mixture was stirred for 10 min after the addition and filtered, affording a yellow solid (8.99 g, 96%). ^{1}H NMR (THF-d_8): δ 8.26 (d, J = 8.6, 1H, H4), 7.75 (s, 1H, H6), 7.36 (d, J = 8.6, 1H, H3), 2.63 (s, 3H, Me).

$(MeOx)_2Zr(CH_2Ph)_2$ (9a). A toluene solution (20 mL) of MeOxH (0.714 g, 4.49 mmol) was added to a toluene solution (100 mL) of $Zr(CH_2Ph)_4$ (1.02 g, 2.25 mmol) dropwise at room temperature over 20 min. The reaction flask was shielded from room light by Al foil. The color of the reaction mixture changed from yellow to orange. After an additional 20 min of stirring, the orange solution was concentrated under vacuum until an orange solid appeared (ca. 10 mL of solution left). The mixture was cooled to −40 °C for 24 h and filtered, which afforded an orange solid (1.09 g, 82.3%). Crystals suitable for X-ray crystallography were obtained by recrystallization from toluene/pentane. Anal. Calcd for $C_{34}H_{30}N_2O_2Zr$: C, 69.23; H, 5.13; N, 4.75. Found: C, 69.06; H, 4.99; N, 5.00. ^{1}H NMR (C_6D_6): δ 7.25 (d, J = 8.3, 2H, H4), 7.24 (t, J = 7.8, 2H, H6), 7.11 (d, J = 7.5, 2H, H5), 6.91 (d, J = 7.6, 4H, *o*-Ph), 6.8 (m, 6H, H7 and *m*-Ph), 6.62 (t, J = 7.1, 2H, *p*-Ph), 6.16 (d, J = 8.3, 2H, H3), 2.65 (d, J = 8.5, 2H, $ZrCH_2$), 2.38 (d, J = 8.5, 2H, $ZrCH_2$), 1.95 (s, 6H, Me). ^{13}C NMR (C_6D_6): δ 161.0, 159.1, 144.3 (*ipso*-Ph), 143.6, 138.2, 128.9, 128.9, 128.7, 127.9, 123.8, 122.1, 115.9, 114.3, 64.0 (J_{CH} = 129 Hz, $ZrCH_2$), 23.2.

$(MeOx)_2Zr(CH_2CMe_3)_2$ (9b). A benzene solution (10 mL) of MeOxH (0.233 g, 1.54 mmol) was added to a pentane solution (30 mL) of $Zr(CH_2CMe_3)_4$ (0.292 g, 0.777 mmol) dropwise over 25 min at room temperature. The bright yellow reaction mixture was stirred for 1 h after the addition, and the solvent was removed under vacuum, yielding 0.390 g (94.8%) of a yellow solid. This product is sufficiently pure for further reactions. The product was recrystallized from toluene/pentane at −40 °C (38.7%). Anal. Calcd for $C_{30}H_{38}N_2O_2Zr$: C, 65.53; H, 6.97; N, 5.10. Found: C, 65.68; H, 6.78; N, 5.32. ^{1}H NMR (C_6D_6): δ 7.24 (m, AB part of ABX, 4H, H5 and H6), 7.12 (d, J = 8.4, 2H, H4), 6.78 (m, X part of ABX, 2H, H7), 6.14 (d, J = 8.4, 2H, H3), 2.5 (s, 6H, *Me*Ox), 2.10 (br d, 2H, $ZrCH_2$), 1.72 (br d, 2H, $ZrCH_2$), 1.23 (s, 18H, CMe_3). ^{13}C NMR (C_6D_6): δ 161.2, 159.4, 143.1, 138.3, 128.7, 128.0, 123.5, 116.5, 114.1, 87.3 ($ZrCH_2$, J_{CH} = 105), 35.4, 34.7, 23.5.

$(MeOx)_2Zr(CH_2SiMe_3)_2$ (9c). A benzene solution (15 mL) of MeOxH (0.210 g, 1.39 mmol) was added to a pentane solution (30 mL) of $Zr(CH_2SiMe_3)_4$ (0.319 g, 0.71 mmol) dropwise over 25 min at room temperature. The yellow-brown reaction mixture was stirred for 1 h after the addition. The solvent was removed under vacuum, yielding a brown solid (0.382 g, 95%). This compound could not be recrystallized due to its high solubility. ^{1}H NMR (C_6D_6): δ 7.21 (m, AB part of ABX, 4H, H5 and H6), 7.11 (d, J = 8.3, 2H, H4), 6.76 (m, X part of ABX, 2H, H7), 6.15 (d, J = 8.4, 2H, H3), 2.55 (s, 6H, *Me*Ox), 1.26 (br d, 4H, $ZrCH_2$), 0.18 (s, 18H, $SiMe_3$). ^{13}C NMR (C_6D_6): 161.0, 159.6, 143.0, 138.5, 128.7, 128.0, 123.6, 116.5, 114.1, 57.9 ($ZrCH_2$, J_{CH} = 103), 23.5, 2.8.

$(MeOx)_2Hf(CH_2Ph)_2$ (10a). A toluene solution (20 mL) of MeOxH (0.601 g, 3.98 mmol) was added to a toluene solution (60 mL) of $Hf(CH_2Ph)_4$ (1.09 g, 2.01 mmol) dropwise over 20 min. The reaction mixture was stirred for 5 min and concentrated under vacuum until a yellow solid appeared (ca. 5 mL of solution left). The mixture was cooled to −40 °C for 24 h and filtered, yielding a yellow solid (1.30 g, 98.5%). ^{1}H NMR (C_6D_6): δ 7.27 (t, J = 7.8, 2H, H6), 7.19 (m, 4H, H4 and H5), 6.90 (d, J = 7.7, 4H, *o*-Ph), 6.76 (m, 6H, H7 and *m*-Ph), 6.48 (t, J = 7.2, 2H, *p*-Ph), 6.10 (d, J = 8.3, 2H, H3), 2.79 (s, 4H, $HfCH_2$), 1.98 (s, 6H, Me). ^{13}C NMR (C_6D_6): δ 161.0, 159.8, 146.3 (*ipso*-Ph), 143.4, 138.6, 129.0, 127.9, 127.7, 127.6, 123.7, 121.0, 116.1, 115.4, 73.9 (J_{CH} = 120, $HfCH_2$), 23.0.

$(MeBr_2Ox)_2Zr(CH_2Ph)_2$ (11a). A toluene solution (60 mL) of $MeBr_2OxH$ (1.88 g, 5.94 mmol) was added to a toluene solution (200 mL) of $Zr(CH_2Ph)_4$ (1.38 g, 3.03 mmol) dropwise over 40 min at room temperature. The reaction flask was shielded from room light with Al foil. The deep orange solution was concentrated under vacuum to 15 mL, cooled to −40 °C for 24 h, and filtered, yielding an orange solid (2.13 g, 79.4%). Anal. Calcd for $C_{34}H_{26}Br_4N_2O_2Zr$: C, 45.10; H, 2.89; N, 3.09. Found: C, 44.99; H, 3.00; N, 3.12. ^{1}H NMR (CD_2Cl_2): δ 8.29 (d, J = 8.6, 2H, H4), 7.93 (s, 2H, H6), 7.13 (d, J = 8.6, 2H, H3), 6.80 (t, J = 7.4, 4H, *m*-Ph), 6.64 (t, J = 7.4, 2H, *p*-Ph), 6.57 (d, J = 7.5, 4H, *o*-Ph), 2.05 (d, J = 8.7, 2H, $ZrCH_2$), 1.99 (s, 6H, Me), 1.86 (d, J = 8.8, 2H, $ZrCH_2$). ^{13}C NMR (CD_2Cl_2): 161.2, 157.2, 143.2, 142.9, 138.7, 134.5, 129.0, 128.8, 126.2, 125.4, 122.5, 108.4 (C5 or C7), 108.2 (C7 or C5), 64.8 (J = 130, $ZrCH_2$), 23.1.

$(MeBr_2Ox)_2Zr(CH_2CMe_3)_2$ (11b). A slurry of $MeBr_2OxH$ (0.872 g, 2.75 mmol) in hexane (25 mL) was added to a hexane solution (50 mL) of $Zr(CH_2CMe_3)_4$ (0.517 g, 1.38 mmol) dropwise over 20 min. The volatiles were removed under vacuum, and the residue was washed with hexanes, yielding a yellow solid (0.888 g, 74.0%). The ^{1}H NMR spectrum indicated that this product was >95% pure **11b**. This sample was used for the dynamic NMR study without further purification. ^{1}H NMR (C_6D_6): δ 7.81 (s, 2H, H6), 7.61 (d, J = 8.6, 2H, H4), 6.02 (d, J = 8.6, 2H, H3), 2.34 (s, 6H, *Me*Br_2Ox), 2.08 (d, J = 13, 2H, $ZrCH_2$), 1.64 (d, J = 13, 2H, $ZrCH_2$), 1.26 (s, 18H, CMe_3). ^{13}C NMR (C_6D_6): δ 161.1, 157.7, 142.8, 138.0, 134.5, 124.5, 108.8, 108.7, 91.0 35.5, 34.7, 23.2.

$(MeBr_2Ox)_4Zr$ (13). A toluene solution (15 mL) of $Zr(CH_2Ph)_4$ (0.540 g, 1.18 mmol) was added to a toluene solution (80 mL) of $MeBr_2OxH$ (1.51 g, 4.76 mmol) at room temperature. The reaction mixture was stirred for 10 min, concentrated to 15 mL under vacuum, and cooled to −40 °C for 12 h. The yellow solid (1.33 g, 83.2%) was collected by filtration and dried under vacuum. ^{1}H NMR (C_6D_6): δ 7.69 (s, 4H, H6), 7.42 (d, J = 8.6, 4H, H4), 6.26 (d, J = 8.6, 4H, H3), 3.54 (s, 12H, Me). ^{13}C NMR (C_6D_6): δ 161.8, 158.2, 143.2, 136.6, 133.7, 125.9, 125.2, 107.2, 106.9, 24.9.

$(MeBr_2Ox)_2Hf(CH_2Ph)_2$ (14a). A toluene solution (50 mL) of $MeBr_2OxH$ (1.17 g, 3.69 mmol) was added to a toluene solution (150 mL) of $Hf(CH_2Ph)_4$ (1.00 g, 1.85 mmol) dropwise over 35 min at room temperature. The orange solution was concentrated to 10 mL under vacuum and cooled to −40 °C for 12 h. The orange solid was isolated by filtration (1.28 g, 75%). Anal. Calcd for $C_{34}H_{26}Br_4N_2O_2Hf$: C, 41.13; H, 2.64; N, 2.82. Found: C, 41.13; H, 2.70; N, 2.72. ^{1}H NMR (C_6D_6): δ 7.85 (s, 2H, H6), 7.75 (d, J = 8.6, 2H, H4), 6.88 (d, J = 7.3, 4H, *o*-Ph), 6.73 (t, J = 7.6, 4H, *m*-Ph), 6.46 (t, J = 7.3, 2H, *p*-Ph), 6.04 (d, J = 8.7, 2H, H3), 2.72 (d, J = 10.9, 2H, $HfCH_2$), 2.63 (d, J = 10.6, 2H, $HfCH_2$), 1.73 (s, 6H, Me). ^{13}C NMR (C_6D_6): δ 161.5, 157.9, 144.6 (*ipso*-Ph), 143.2, 138.4, 134.9, 128.3, 128.0, 126.1, 125.0, 121.9, 110.0, 108.5, 75.3 (J_{CH} = 122, $HfCH_2$), 22.7.

(66) (a) Zucchini, U.; Albizzati, E.; Giannini, U. *J. Organomet. Chem.* **1971**, *26*, 357. (b) Davidson, P. J.; Lappert, M. F.; Pearce, R. *J. Organomet. Chem.* **1973**, *57*, 269.

$(MeOx)_2ZrCl_2$ (15). Ether (50 mL) was added to a solid mixture of $ZrCl_4$ (2.50 g, 10.7 mmol) and (MeOx)Li (**2-Li**) (3.60 g, 20.2 mmol) at room temperature. The reaction mixture was stirred for 2 days and the solvent was removed under vacuum, yielding a yellow solid. The ^{1}H NMR spectrum indicated that this material contained **15** as the major MeOx product (ca. 90%). ^{1}H NMR (CD_2Cl_2): δ 8.05 (d, J = 8.3, 2H, H4), 7.45 (t, J = 7.8, 2H, H6), 7.23 (dd, J = 8.2, 1.1, 2H, H5), 7.20 (d, J = 8.5, 2H, H3), 7.05 (dd, J = 7.6, 1.1, 2H, H7), 3.06 (s, 6H, Me). This material was used directly without isolation from LiCl due to its low solubility. The identity of **15** was confirmed by an alternate synthesis. A toluene solution (15 mL) of MeOxH (0.152 g, 1.01 mmol) was added to a toluene solution (25 mL) of $Zr(CH_2Ph)_4$ (0.232 g, 0.509 mmol) dropwise over 10 min. The solution was stirred for 10 min, and solid $[HNMe_3]Cl$ (0.095 g, 0.994 mmol) was added. The mixture was stirred for 12 h, cooled to −40 °C for 12 h, and filtered, yielding a yellow solid (0.175 g, 76.1%). The ^{1}H NMR spectrum of this material was identical to that prepared from (MeOx)Li and $ZrCl_4$.

$(MeBr_2Ox)_2ZrCl_2$ (16). Ether (80 mL) was added to a solid mixture of $(MeBr_2Ox)Li$ (**3-Li**) (2.96 g, 9.15 mmol) and $ZrCl_4$ (1.05 g, 4.49 mmol). The reaction mixture was stirred for 2 days at room temperature, and the solvent was removed under vacuum, yielding a yellow solid. The ^{1}H NMR spectrum indicated that this material contained **16** as the major $MeBr_2$-Ox containing product (>90%). This material was used directly without further purification due to its low solubility.

An analytically pure sample of **16** was obtained by the following route. Methylene chloride (20 mL) was added to a solid mixture of $(MeBr_2Ox)_2Zr(CH_2Ph)_2$ (0.523 g, 0.578 mmol) and $[HNMe_3]Cl$ (0.092 g, 0.96 mmol) at room temperature. The reaction mixture was stirred for 30 min and concentrated under vacuum to 10 mL, and benzene (10 mL) was added. The yellow solid (0.312 g, 70%) was collected by filtration and dried under vacuum. Anal. Calcd for $C_{20}H_{12}Br_4Cl_2N_2O_2Zr$: C, 30.24; H, 1.52; N, 3.53; Cl, 8.93. Found: C, 30.08; H, 1.44; N, 3.41; Cl, 9.10. ^{1}H NMR (CD_2Cl_2): δ 8.35 (d, J = 8.6, 2H, H4), 7.95 (s, 2H, H6), 7.36 (d, J = 8.6, 2H, H3), 3.11 (s, 6H, Me).

$(MeBr_2Ox)_2Zr(NMe_2)_2$ (17). An ether slurry (80 mL) of $(MeBr_2Ox)_2ZrCl_2$ (**16**, 2.33 mmol) was generated by the reaction of $ZrCl_4$ (0.540 g, 2.33 mmol) and $(MeBr_2Ox)Li$ (**3-Li**, 1.50 g, 4.66 mmol) as described above. Solid $LiNMe_2$ (0.256 g, 5.02 mmol) was added at room temperature. The brown reaction mixture was stirred for 5 h at room temperature, and the solvent was removed under vacuum. The residue was taken up in benzene (80 mL) and filtered. The solvent was removed from the filtrate under vacuum, yielding a tan solid (1.54 g, 81.5%). Anal. Calcd for $C_{24}H_{24}Br_4N_4O_2Zr$: C, 35.53; H, 2.98; N, 6.90. Found, C, 35.11; H, 2.79; N, 4.90 (duplicate analysis also gave a low %N value, 5.6%). ^{1}H NMR (C_6D_6): δ 7.82 (s, 2H, H6), 7.61 (d, J = 8.6, 2H, H4), 6.13 (d, J = 8.6, 2H, H3), 3.30 (s, 12H, NMe_2), 2.52 (s, 6H, *Me*Br_2Ox). ^{13}C NMR (C_6D_6): δ 161.0, 157.9, 143.1, 137.7, 134.4, 126.2, 124.5, 108.5, 107.1, 44.0, 23.5.

Generation of $(MeBr_2Ox)AlMe_2$ (18). A hexane slurry (20 mL) of $MeBr_2OxH$ (1.59 g, 5.03 mmol) was added to a hexane solution (3 mL) of $AlMe_3$ (6 mmol) at room temperature. A yellow precipitate formed. The mixture was stirred for 20 min and filtered, yielding a yellow solid (1.41 g, 74.9%). The ^{1}H NMR spectrum indicated that this material contains 87% $(MeBr_2Ox)AlMe_2$ and 13% $(MeBr_2Ox)_2AlMe$.[67] ^{1}H NMR (CD_2Cl_2): δ 8.53 (d, J = 8.6, 1H, H4), 7.91 (s, 1H, H6), 7.55 (d, J = 8.6, 1H, H3), 2.86 (s, 3H, *Me*Br_2Ox), −0.58 (s, 6H, $AlMe_2$). ^{13}C NMR (CD_2Cl_2): δ 159.5, 158.2, 141.0, 139.7, 135.7, 129.3, 124.8, 109.7, 105.2, 23.1, −10.5 (br, AlMe, J_{CH} = 104).

Thermal Rearrangement of 11a to 19. A toluene solution (80 mL) of $(MeBrOx)_2Zr(CH_2Ph)_2$ (0.950 g) was stirred for 1.5 h at 60 °C. The volatiles were removed under vacuum, leaving a brown sticky residue, which was extracted with a mixture of benzene and pentane (40 mL, ca. 3/2 by volume). The extract was evaporated to dryness under vacuum, yielding a brown solid (0.419 g, 44.1%; ca. 90% **19** and 10% **11a** by ^{1}H NMR). A portion (0.267 g) of this material was dissolved in toluene (5 mL), and the solution was layered with hexane (20 mL) and cooled to −40 °C for 24 h. The yellow solid which formed was collected by filtration and dried under vacuum (0.123 g, 46.1% recrystallization yield). The ^{1}H NMR spectrum established that this material contains 1 equiv of toluene vs **19**. Anal. Calcd for $C_{34}H_{26}Br_4N_4O_2Zr\cdot C_7H_8$: C, 49.36; H, 3.44; N, 2.81. Found: C, 47.33; H, 3.24; N, 3.22 (the low %C values may be due to toluene loss during analysis). ^{1}H NMR (CD_2Cl_2): δ 8.37 (d, J = 8.7, 1H, H4), 7.99 (s, 1H, H6 or H6′), 7.50 (s, 1H, H6′ or H6), 7.15 (d, J = 8.9, 1H, H3), 7.05 (m, 3H, *p*-Ph′ and *m*-Ph′), 6.83 (d, J = 6.6, 2H, *o*-Ph′), 6.74 (d, J = 9.8, 1H, H4′), 6.69 (t, J = 7.7, 2H, *m*-Ph), 6.57 (t, J = 6.9, 1H, *p*-Ph), 6.29 (d, J = 7.2, 2H, *o*-Ph), 4.99 (d, J = 9.4, 1H, H3′), 3.31 (d, J = 12.2, 1H, CH_2Ph′), 2.86 (d, J = 11.8, 1H, CH_2Ph), 2.84 (d, J = 11.8, 1H, CH_2Ph), 2.32 (d, J = 13, 1H, CH_2Ph′), 2.07 (s, 3H, *Me*Br_2Ox), 0.62 (s, 3H, *Me*Br_2Ox′). ^{13}C NMR (CD_2Cl_2): δ 163.0, 156.3, 149.5, 145.3, 142.1, 139.5, 138.2, 136.4, 135.2, 134.9, 131.7, 127.7, 127.6, 126.5, 126.4, 126.3, 126.1, 125.6, 125.5, 123.9, 121.6, 115.8, 113.5, 110.0, 109.0, 73.6 (*C*H_2Ph, J_{CH} = 116), 61.5 (C2′), 48.3 (*C*H_2Ph′, J_{CH} = 126), 25.2, 25.1; one *ipso* C resonance not observed.

$[(MeOx)_2Zr(CH_2Ph)][B(C_6F_5)_4]$ (20a). A mixture of $(MeOx)_2Zr(CH_2Ph)_2$ (**9a**, 0.298 g, 0.517 mmol) and $[HNMePh_2][B(C_6F_5)_4]$ (0.438 g, 0.507 mmol) in benzene (5 mL) was stirred at room temperature for 5 min. A brown oil separated. The supernatant was decanted from the oil. The oil was washed with benzene (5 mL) and dried under vacuum, yielding a brown solid (0.442 g, 75.1%). ^{1}H NMR (CD_2Cl_2): δ 8.42 (d, J = 8.4, 1H, H4), 8.41 (d, J = 7.5, 1H, H7), 8.32 (d, J = 8.4, 1H, H4′), 7.87 (t, J = 7.8, 1H, H6), 7.80 (d, J = 7.1, 1H, H5), 7.71 (t, J = 8.1, 1H, H6′), 7.53 (m, 2H, H5′, H7′), 7.32 (d, J = 8.3, 1H, H3), 7.00 (t, J = 7.7, 2H, *m*-Ph), 6.93 (d, J = 6.8, 2H, *o*-Ph), 6.82 (d, J = 8.3, 1H, H3′), 6.72 (t, J = 6.8, 1H, *p*-Ph), 3.64 (d, J = 9.5, 1H, $ZrCH_2$), 3.29 (d, J = 9.7, 1H, $ZrCH_2$), 1.95 (s, 3H, Me), 0.56 (s, 3H, Me′). ^{13}C NMR (CD_2Cl_2): δ 160.8, 160.5, 155.1, 151.8, 148.6 (d, J_{CF} = 241, $B(C_6F_5)_4^-$), 143.3, 143.2, 143.0, 139.5, 138.6 (d, J_{CF} = 243, $B(C_6F_5)_4^-$), 137.2, 136.7 (d, J_{CF} = 243, $B(C_6F_5)_4^-$), 132.0, 130.3, 130.2, 129.2, 128.8, 128.5, 127.9, 125.8, 124.9, 124.8, 124.0 (br, $B(C_6F_5)_4^-$), 121.9, 120.2, 116.3, 82.0 (J_{CH} = 132, $ZrCH_2$), 24.1, 22.7.

$[(MeOx)_2Zr(CH_2CMe_3)][B(C_6F_5)_4]$ (20b). A mixture of $(MeOx)_2Zr(CH_2CMe_3)_2$ (**9b**, 0.105 g, 0.197 mmol) and $[HNMePh_2][B(C_6F_5)_4]$ (0.163 g, 0.189 mmol) in benzene was stirred for 15 min at room temperature. A brown oil separated. The supernatant was removed by pipette, and the residue was washed with benzene (2 mL) and dried under vacuum, yielding a yellow solid (0.205 g, 87.4%). ^{1}H NMR (CD_2Cl_2): δ 8.77 (d, J = 7.6, 1H, H7), 8.65 (d, J = 8.5 Hz, 1H, H4), 8.31 (d, J = 8.3, 1H, H4′), 8.04 (t, J = 8.0, 1H, H6), 7.97 (d, J = 7.7, 1H, H5), 7.72 (t, J = 7.9, 1H, H6′), 7.60 (m, 3H, H3, H5′, H7′), 6.74 (d, J = 8.3, 1H, H3′), 2.62 (d, J = 11.3, 1H, $ZrCH_2$), 2.60 (s, 3H, *Me*Ox), 2.40 (d, J = 11.4, 1H, $ZrCH_2$), 0.76 (s, 9H, CMe_3), 0.46 (s, 3H, *MeOx*′). ^{13}C NMR (CD_2Cl_2): δ 160.9, 160.3, 154.7, 151.7, 148.5 (d, J_{CF} = 241, $B(C_6F_5)_4^-$), 144.7, 143.1, 143.0, 138.6 (d, J_{CF} = 243, $B(C_6F_5)_4^-$), 136.7, 136.6 (d, J_{CF} = 243, $B(C_6F_5)_4^-$), 130.7, 130.4, 128.6, 125.7, 125.4, 125.0, 124.0 (br, $B(C_6F_5)_4^-$), 122.1, 119.9, 118.1 (J_{CH} = 100, $ZrCH_2$), 116.7, 39.4, 32.5, 24.3, 22.2; one aromatic carbon was not observed.

$[(MeBr_2Ox)_2Zr(CH_2Ph)(NMe_2Ph)][B(C_6F_5)_4]$ (21a). An NMR tube was charged with $(MeBr_2Ox)_2Zr(CH_2Ph)_2$ (**11a**, 14.9 mg, 0.016 mmol) and $[HNMe_2Ph][B(C_6F_5)_4]$ (12.1 mg, 0.015 mmol), and CD_2Cl_2 (0.5 mL) was added by vacuum transfer at −78 °C. The NMR tube was maintained at −78 °C. A clear yellow solution formed within 5 min. The ^{1}H NMR spectrum was recorded at −40 °C and indicated that **21a** was formed quantitatively. ^{1}H NMR (CD_2Cl_2, −40 °C): δ 8.43 (d, J = 8.6,

(67) ^{1}H NMR data for $(MeBr_2Ox)_2AlMe$ (CD_2Cl_2): δ 8.44 (d, J = 8.6 Hz, 2H, H4), 7.84 (s, 2H, H6), 7.60 (d, J = 8.7 Hz, 2H, H3), 3.19 (s, 6H, Me), −0.66 (s, 3H, AlMe).

1H, H4), 8.36 (d, J = 8.6, 1H, H4), 8.09 (s, 1H, H6), 8.08 (s, 1H, H6), 7.4−6.7 (m, 12H, H3 and Ph), 3.46 (s, 3H, NMe_2Ph), 3.16 (d, J = 9.1, 1H, $ZrCH_2$), 3.10 (d, J = 9.1, 1H, $ZrCH_2$), 3.00 (s, 3H, NMe_2Ph), 1.64 (s, 3H, $MeBr_2Ox$), 1.36 (s, 3H, $MeBr_2Ox$). The room-temperature ^{1}H NMR spectrum of this compound contains broad resonances characteristic of NMe_2-Ph exchange, as described in the text.

[(MeBr$_2$Ox)$_2$Hf(CH$_2$Ph)(NMe$_2$Ph)][B(C$_6$F$_5$)$_4$]. An NMR tube was charged with $(MeBr_2Ox)_2Zr(CH_2Ph)_2$ (**14a**, 22.6 mg, 0.0228 mmol) and $[HNMe_2Ph][B(C_6F_5)_4]$ (19.5 mg, 0.0243 mmol), and CD_2Cl_2 (0.5 mL) was added by vacuum transfer to yield a yellow solution. The ^{1}H NMR spectrum was recorded at −40 °C and established that the formation of $(MeBr_2Ox)_2Hf(CH_2Ph)(NMe_2Ph)^+$ was quantitative. ^{1}H NMR (CD_2Cl_2, −40 °C): δ 8.46 (d, J = 8.6, 1H, H4), 8.38 (d, J = 8.5, 1H, H4), 8.12 (s, 1H, H6), 8.10 (s, 1H, H6), 7.8−6.2 (m, 12H, H3 and Ph), 3.92 (s, 3H, NMe_2Ph), 3.78 (s, 3H, NMe_2Ph), 2.73 (d, J = 11.3, 1H, $HfCH_2$), 2.43 (d, J = 11.3, 1H, $HfCH_2$), 1.60 (s, 3H, MeBr$_2$Ox), 1.46 (s, 3H, MeBr$_2$Ox). The room-temperature ^{1}H NMR spectrum contains broad resonances characteristic of NMe_2-Ph exchange.

[(MeOx)$_2$Hf(CH$_2$Ph)][B(C$_6$F$_5$)$_4$] (22a). A mixture of $(MeOx)_2Hf(CH_2Ph)_2$ (**10a**, 0.141 g, 0.208 mmol) and $[HNMePh_2][B(C_6F_5)_4]$ (0.171 g, 0.198 mmol) in benzene (3 mL) was stirred for 10 min at room temperature. A yellow oil separated. The supernatant was removed by pipette, and the oil was washed with benzene (3 mL) and dried under vacuum, yielding a yellow solid (0.205 g, 80.4%). The ^{1}H NMR spectrum indicated that this material contains 0.4 equiv of occluded benzene. Anal. Calcd for $C_{51}H_{23}BF_{20}N_2O_2Hf\cdot0.4C_6H_6$: C, 49.48; H, 1.97; N, 2.16. Found: C, 49.42; H, 1.78; N, 2.31. ^{1}H NMR (CD_2Cl_2): δ 8.56 (dd, J = 7.8, 1.2, 1H, H7), 8.48 (d, J = 8.5, 1H, H4), 8.34 (d, J = 8.3, 1H, H4′), 7.92 (t, J = 7.9, 1H, H6), 7.86 (dd, J = 8.3, 1.1, 1H, H5), 7.75 (t, J = 7.9, 1H, H6′), 7.54 (m, 2H, H5′ and H7′), 7.36 (d, J = 8.5, 1H, H3), 7.01 (t, J = 7.8, 2H, *m*-Ph), 6.85 (d, J = 8.3, 1H, H3′), 6.80 (d, J = 7.1, 2H, *o*-Ph), 6.67 (t, J = 7.4, 1H, *p*-Ph), 3.24 (d, J = 11.3, 1H, $HfCH_2$), 2.90 (d, J = 11.3, 1H, $HfCH_2$), 1.96 (s, 3H, Me), 0.53 (s, 3H, Me′). ^{13}C NMR (CD_2Cl_2): δ 161.4, 161.2, 154.5, 150.2, 148.5 (d, J_{CF} = 240, $B(C_6F_5)_4^-$), 143.8, 143.4, 142.9, 140.0, 138.5 (d, J_{CF} = 243, $B(C_6F_5)_4^-$), 136.2 (d, J_{CF} = 243, $B(C_6F_5)_4^-$), 136.0, 130.6, 130.6, 130.4, 129.5, 128.7, 128.1, 127.5, 126.2, 125.7, 125.1, 121.9, 120.7, 117.9, 81.7 (J_{CH} = 125, $HfCH_2$), 23.8, 22.5; the $B(C_6F_5)_4^-$ *ipso*-carbon was not observed. ^{19}F NMR (CD_2Cl_2) δ −132.9 (8F), −163.4 (4F), −167.3 (8F). ^{19}F NMR (CD_2Cl_2, −90 °C): δ −133.4 (8F), −162.0 (4F), −166.0 (8F).

[(MeBr$_2$Ox)$_2$Zr(CH$_2$Ph)][B(C$_6$F$_5$)$_4$] (23a). Benzene (7 mL) was added to a solid mixture of $(MeBr_2Ox)_2Zr(CH_2Ph)_2$ (**11a**, 0.451 g, 0.498 mmol) and $[HNMePh_2][B(C_6F_5)_4]$ (0.428 g, 0.496 mmol), and the mixture was stirred for 10 min. A brown oil separated. The supernatant was removed by pipette, and the oil was washed with benzene (10 mL) and dried under vacuum, yielding a yellow solid. The ^{1}H NMR spectrum established that this material contained 1.4 equiv of occluded benzene. Crystals of **23a** suitable for X-ray diffraction were obtained by recrystallization from CH_2Cl_2 at −40 °C. Anal. Calcd for $C_{51}H_{19}BBr_4F_{20}N_2O_2Zr\cdot1.4C_6H_6$: C, 44.51; H, 1.72; N, 1.75. Found: C, 44.04; H, 1.78; N, 1.72. ^{1}H NMR (CD_2Cl_2): δ 8.71 (d, J = 8.6, 2H, H4), 8.06 (s, 2H, H6), 7.73 (d, J = 8.7, 2H, H3), 6.9 (br, 2H, *o*-Ph), 6.86 (t, J = 7.5, *p*-Ph), 3.56 (d, J = 8.7, 1H, $ZrCH_2$), 3.46 (d, J = 8.8, 1H, $ZrCH_2$), 3.16 (s, 6H, Me); the *m*-Ph resonance is not observed at room temperature. ^{1}H NMR (CD_2Cl_2, −85 °C): δ 8.71 (d, J = 8.4, 1H, H4), 8.51 (d, J = 8.3, 1H, H4), 7.98 (s, 1H, H6), 7.95 (s, 1H, H6), 7.82 (d, J = 8.6, 1H, H3), 7.71 (t, J = 7.3, 1H, *m*-Ph), 7.59 (d, J = 8.9, 1H, H3), 7.00 (d, J = 7.2, 1H, *o*-Ph), 6.77 (d, J = 7.9, 1H, *o*-Ph), 6.72 (t, J = 7.4, 1H, *p*-Ph), 6.60 (t, J = 7.6, 1H, *m*-Ph), 3.55 (d, J = 8.4, 1H, $ZrCH_2$), 3.41(d, partially obscured, 1H, $ZrCH_2$), 3.38 (s, 3H, Me), 2.83 (s, 3H, Me). ^{13}C NMR (CD_2Cl_2): δ 164.0, 152.8, 148.5 (d, J_{CF} = 240, $B(C_6F_5)_4^-$), 143.4, 142.2, 138.6 (d, J_{CF} = 243, $B(C_6F_5)_4^-$), 136.6 (d, J_{CF} = 243, $B(C_6F_5)_4^-$), 135.4, 134.9, 130.6, 126.8, 126.8, 124.0 (br, $B(C_6F_5)_4^-$), 112.7, 110.0, 77.7 (J_{CH} = 145, $ZrCH_2$), 26.1; two aromatic carbons were not observed. ^{11}B NMR (CD_2Cl_2): δ −15.2. ^{19}F NMR (CD_2Cl_2, −50 °C): δ −133.4 (8F), −162.5 (4F), −166.6 (8F).

[(MeBr$_2$Ox)$_2$Hf(CH$_2$Ph)][B(C$_6$F$_5$)$_4$] (24a). Benzene (3 mL) was added to a solid mixture of $(MeBr_2Ox)_2Hf(CH_2Ph)_2$ (**14a**, 0.302 g, 0.304 mmol) and $[HNMePh_2][B(C_6F_5)_4]$ (0.261 g, 0.302 mmol) at room temperature. The reaction mixture was stirred for 10 min, and a brown oil separated. The supernatant was removed by pipette, and the oil was washed with benzene (3 mL) and dried under vacuum, yielding a yellow solid (0.276 g, 92.1%). The ^{1}H NMR spectrum indicated that this material contained 1.2 equiv of occluded benzene. Anal. Calcd for $C_{51}H_{19}BBr_4F_{20}N_2O_2Hf\cdot1.2C_6H_6$: C, 41.75; H, 1.58; N, 1.67. Found: C, 41.67; H, 1.81; N, 1.67. ^{1}H NMR (CD_2Cl_2): δ 8.73 (d, J = 8.6, 2H, H4), 8.09 (s, 2H, H6), 7.76 (d, J = 8.7, 2H, H3), 7.19 (br s, 2H, *m*-Ph), 6.98 (d, J = 7.2, 2H, *o*-Ph), 6.79 (t, J = 7.5, 1H, *p*-Ph), 3.22 (s, 6H, Me), 3.19 (d, partially obscured, 1H, $HfCH_2$), 3.08 (d, J = 10.2, 1H, $HfCH_2$). ^{1}H NMR (−85 °C): δ 8.65 (s br, 2H, H4), 8.00 (s, 2H, H6), 7.72 (br s, 2H, H3), 7.68 (t, J = 7.1, 1H, *m*-Ph), 7.15 (d, J = 7.1, 1H, *o*-Ph), 6.72 (d, J = 7.6, 1H, *o*-Ph), 6.67 (t, J = 7.3, 1H, *p*-Ph), 6.54 (t, J = 7.6, 1H, *m*-Ph), 3.5 (br s, 3H, Me), 3.19 (d, J = 10.0, $HfCH_2$), 3.00 (d, J = 10.0, $HfCH_2$), 2.9 (br s, 3H, Me). ^{13}C NMR (CD_2Cl_2): δ 164.9, 152.1, 148.5 (d, J_{CF} = 241, $B(C_6F_5)_4^-$), 143.2, 142.5, 138.6 (d, J_{CF} = 244, $B(C_6F_5)_4^-$), 136.7 (d, J_{CF} = 243, $B(C_6F_5)_4^-$), 135.7, 135.5, 134.5, 131.1, 130.4, 127.1, 126.8, 124.0 (br), 112.7, 111.2, 77.0 (J_{CH} = 143, $HfCH_2$), 26.2.

[(MeBr$_2$Ox)$_2$Zr(CH$_2$Ph)(PMe$_3$)][B(C$_6$F$_5$)$_4$] (25a). Benzene (1.5 mL) was added to a solid mixture of $(MeBr_2Ox)_2Zr(CH_2Ph)_2$ (**11a**, 0.332 g, 0.367 mmol) and $[HNMePh_2][B(C_6F_5)_4]$ (0.314 g, 0.364 mmol), and the mixture was stirred at room temperature for 10 min. A yellow oil separated. The supernatant was removed by pipette, and benzene (2 mL) was added to the yellow oily residue. This mixture was exposed to PMe_3 (210 mmHg) on a vacuum line for 15 min. The solvent and excess PMe_3 were removed under vacuum, yielding a yellow solid (0.490 g, 86.7%). An analytically pure sample was obtained by washing this product with benzene and drying under vacuum. Anal. Calcd for $C_{54}H_{28}BBr_4F_{20}N_2O_2PZr$: C, 41.32; H, 1.80; N, 1.79. Found: C, 41.51; H, 1.89; N, 1.69. ^{1}H NMR (CD_2Cl_2): δ 8.57 (d, J = 8.6, 1H, H4), 8.43 (d, J = 8.6, 1H, H4′), 8.07 (s, 1H, H6 or H6′), 8.03 (s, 1H, H6 or H6′), 7.47 (t, J = 7.6, 1H, *m*-Ph), 7.40 (d, J = 8.5, 1H, H3), 7.29 (d, J = 8.7, 1H, H3′), 7.25 (d, J = 7.5, 1H, *o*-Ph), 6.52 (d, J = 7.6, 1H, *o*-Ph), 6.51 (t, J = 7.4, 1H, *p*-Ph), 6.31 (t, J = 7.5, 1H, *m*-Ph), 3.50 (dd, J = 9.4, 7.5, 1H, $ZrCH_2$), 3.29 (dd, J = 7.5, 5.0, 1H, $ZrCH_2$), 2.25 (s, 3H, MeBr$_2$Ox), 2.02 (s, 3H, Me'Br$_2$Ox), 1.26 (d, J_{PH} = 8.0, 9H, PMe_3). ^{13}C NMR (CD_2Cl_2): δ 163.5, 160.9, 154.4, 153.9, 148.5 (d, J_{CF} = 238, $B(C_6F_5)_4^-$), 143.3, 142.9, 141.3, 140.9, 138.5 (d, J_{CF} = 243, $B(C_6F_5)_4^-$), 136.7 (d, J_{CF} = 243, $B(C_6F_5)_4^-$), 135.6, 135.5, 135.4, 134.2, 132.2, 132.1, 130.2, 129.8, 127.0, 126.3, 126.2, 126.0, 124.0 (br, $B(C_6F_5)_4^-$), 111.9, 110.8, 110.2, 109.9, 70.7 (J_{PC} = 9, J_{CH} = 145, $ZrCH_2$), 24.1, 23.8, 13.5 (J_{PC} = 21.0, PMe_3).

[(MeBr$_2$Ox)$_2$Hf(CH$_2$Ph)(PMe$_3$)][B(C$_6$F$_5$)$_4$] (26a). A mixture of $[(MeBr_2Ox)_2Hf(CH_2Ph)][B(C_6F_5)_4]$ (0.140 g, 0.089 mmol) in benzene (3 mL) was exposed to PMe_3 (150 mm Hg) on a vacuum line for 15 min, with stirring at room temperature. The volatiles were removed under vacuum, yielding a yellow solid (0.105 g, 71.6%) which was shown by ^{1}H NMR to be >95% pure **26a**. ^{1}H NMR (CD_2Cl_2): δ 8.59 (d, J = 8.6, 1H, H4), 8.44 (d, J = 8.6, 1H, H4′), 8.11 (s, 1H, H6 or H6′), 8.07 (s, 1H, H6 or H6′), 7.41 (d, J = 8.7, 1H, H3), 7.29 (d, J = 8.6, 1H, H3′), 6.45 (t, J = 7.6, 1H, *p*-Ph), 3.16 (dd, J = 8, 5, 1H, $HfCH_2$), 2.98 (dd, J = 8, 2, 1H, $HfCH_2$), 2.24 (s, 3H, MeBr$_2$Ox), 1.99 (s, 3H, Me'Br$_2$Ox), 1.29 (d, J_{PH} = 8.2, 9H, PMe_3); the *m*-Ph and *o*-Ph resonances are not observed at room temperature due to the η^2−η^1 benzyl isomerization. ^{1}H NMR (CD_2Cl_2, −50 °C): δ 8.52 (d, J = 8.6, 1H, H4), 8.36 (d, J = 8.6, 1H , H4′), 8.03 (s, 1H, H6 or H6′), 7.97 (s, 1H, H6 or H6′), 7.39 (m, 3H, H3, *o*-Ph and *m*-Ph), 7.28 (d, J = 8.7, 1H, H3′), 6.47 (d, J = 7.0, 1H, *o*-Ph), 6.36 (t, J = 7.0, 1H, *p*-Ph), 6.15 (t, J = 7.0, 1H, *m*-Ph),

Table 5. Summary of Crystallographic Data

cmpd	$(MeOx)_2Zr(CH_2Ph)_2$ (**9a**)	$[(MeBr_2Ox)_2Zr(\eta^2\text{-}CH_2Ph)][B(C_6F_5)_4]$ (**23a**)
empirical formula	$C_{34}H_{30}N_2O_2Zr$	$C_{51}H_{19}BBr_4F_{20}N_2O_2Zr$
fw	589.85	1493.4
cryst size (mm)	0.44 × 0.38 × 0.12	0.09 × 0.40 × 0.63
color/shape	orange/prism	orange/hexagonal plate
space group	$P\bar{1}$	$P2_1/c$
a (Å)	10.802(2)	12.638(3)
b (Å)	13.767(3)	19.034(3)
c (Å)	10.332(2)	20.872(4)
α (deg)	74.92(2)	90
β (deg)	99.34(2)	97.77(2)
γ (deg)	104.15(2)	90
V (Å^3)	1430.5(9)	5020(3)
Z	2	4
temperature (K)	293	200
diffractometer	Enraf-Nonius CAD-4	Enraf-Nonius CAD-4
radiation, λ	Mo Kα, 0.710 73 Å	Mo Kα, 0.710 73 Å
monochromator	graphite	graphite
2θ range (deg)	$4 < 2\theta < 50$	$4 < 2\theta < 55$
data collected h, k, l	−12 to 3, −15 to 16, −12 to 12	−16 to 1, −24 to 6, −27 to 27
total no. of reflns collected	5784	16909
no of unique reflns	4900	11431
R_{int}	0.023	0.030
no. of obs reflns, criterion	3709, $I > 2\sigma(I)$	6619, $I > 2\sigma(I)$
μ (cm^{-1})	4.08	34.85
abs corr factors (min/max)	1.00/1.52	1.000/1.880
abs corr method	ψ scans	ψ scans
structure soln[a]	direct methods	direct methods
refinement[b]	FMLS on F, non-H anisotropic; H isotropic	FMLS on F, non-H anisotropic; H47A, H47B isotropic; other H calculated
total no. of params	472	738
weighting scheme[c]	$p = 0.02$, $q = 0.0$	$p = 0.03$, $q = 0.0$
R[d]	0.044	0.0382
R_w[e]	0.049	0.0475
GOF	1.53	1.11
max resid density (e/Å^3)	0.77	0.73
max shift/ESD	0.05	0.09

[a] MULTAN (Main, P.; Fiske, S. J.; Hull, S. E.; Lessinger, L.; Germain, G.; DeClercq, J. P.; Woolfson, M. M.; *Multan80*; University of York: York, U.K., 1980). [b] Data processing and refinement with MolEN (Fair, C. K.; *MolEN Users Manual*; Enraf-Nonius: Delft, Netherlands, 1990); scattering factors taken from *International Tables for X-Ray Crystallography*; The Kynoch Press: Birmingham, U.K., 1970; Vol. II. [c] $w = [(\sigma_F)^2 + (pF)^2 + q]^{-1}$. Killean, R. C. G.; Lawrence, J. L. *Acta. Crystallogr., Sect. B* **1969**, *B25*, 1750. [d] $R = \sum(|F_o| - |F_c|)/\sum F_o$. [e] $R_w = \{[\sum(F_o - F_c)^2]/[\sum w(F_o)^2]\}^{1/2}$.

3.10 (t, J = 9, 1H, $HfCH_2$), 2.86 (dd, J = 9, 4, 1H, $HfCH_2$), 2.17 (s, 3H, *Me*Br_2Ox), 1.93 (s, 3H, *Me*Br_2Ox′), 1.22 (d, J = 8, 9H, PMe_3). ^{13}C NMR (CD_2Cl_2): δ 163.7, 161.5, 154.3, 154.1, 148.5 (d, J_{CF} = 242, $B(C_6F_5)_4^-$), 143.2, 143.1, 141.4, 141.0, 138.5 (d, J_{CF} = 242, $B(C_6F_5)_4^-$), 136.6 (d, J_{CF} = 243, $B(C_6F_5)_4^-$), 135.8, 135.6, 132.2 (br), 131.7, 130.1, 127.0, 126.5, 126.4, 126.1, 124.0 (br, $B(C_6F_5)_4^-$), 111.7, 111.4, 111.2, 110.7, 71.8 (J_{PC} = 4, J_{CH} = 141, $HfCH_2$), 24.0, 23.7, 13.2 (J_{PC} = 23, PMe_3); one aromatic resonance was not observed.

Ethylene Polymerization. Polymerization conditions and results are summarized in Table 3. Entries 1−11 refer to reactions which were performed in a Fischer−Porter apparatus. In several cases, as summarized in Table 3, multiple runs were performed to determine the reproducibility of the yields and activities. A solution of the $[(Ox)_2MR][B(C_6F_5)_4]$ "active catalyst" was generated from the catalyst and cocatalyst as indicated in Table 3 and exposed to 2−3 atm of ethylene at the desired temperature for 30 min. The polymerization was quenched with acidic MeOH, and the polymer was collected by filtration, washed with MeOH, and dried under vacuum. Runs 12−15 were performed in a 1 L autoclave. For runs 12, 13, and 15, the solvent, $Al(^iBu)_3$, the catalyst, and the cocatalyst were introduced to the reactor in that order under 8 atm of ethylene. For run 14, the solvent, MAO, and **16** were introduced to the reactor in that order under 8 atm of ethylene.

X-ray Crystallography. Experimental data for the X-ray diffraction analyses of **9a** and **23a** are summarized in Table 5.

Acknowledgment. This work was supported by the Mitsubishi Chemical Corporation and the Department of Energy (Grant No. DE-FG02-88ER13935).

Supporting Information Available: Tables of atomic coordinates and equivalent isotropic displacement parameters, anisotropic displacement parameters, bond distances, bond angles, and hydrogen atom coordinates and isotropic displacement parameters for **9a** and **23a** (25 pages). Ordering information is given on any current masthead page.

OM970235S